

THESIS

PROBING UNCONVENTIONAL VESICULAR TRAFFICKING WITH K63-  
POLYUBIQUITIN SENSORS

Submitted by

Sharon Lian

Department of Biochemistry and Molecular Biology

In partial fulfillment of the requirements

For the Degree of Master of Science

Colorado State University

Fort Collins, Colorado

Summer 2019

Master's Committee:

Advisor: Robert Cohen

Co-Advisor: Tingting Yao

Noreen Reist

Copyright by Sharon Lian 2019

All Rights Reserved

## ABSTRACT

### PROBING UNCONVENTIONAL VESICULAR TRAFFICKING WITH K63-POLYUBIQUITIN SENSORS

For signaling purposes, the small protein ubiquitin (Ub) acts as a post-translational modification. Ub can polymerize with diverse Ub-Ub chain linkages which are involved in numerous cellular mechanisms. To investigate processes mediated by a particular Ub linkage, tools selective against specific forms of polyUb are useful. Vx3 is a previously developed sensor that specifically binds K63-linked polyUb with high affinity and acts as a competitive inhibitor by blocking K63-polyUb-dependent signaling. When expressed in cells, Vx3 forms stable cytoplasmic foci that co-localize with autophagy related protein 9A (ATG9A) and late endosomal/lysosomal markers. However, Vx3 foci only co-localize with the autophagy marker LC3 upon selective autophagy induction. Proteins associated with Vx3 were identified through Vx3 co-immunoprecipitation and mass spectrometry analysis. The most abundant were plasma membrane proteins including transferrin receptor (TfR) and major histocompatibility complex I (MHC-I), which co-localized into cytoplasmic foci with Vx3. Biochemical and confocal microscopy analyses revealed that TfR at Vx3 foci is K63-polyubiquitinated, originated from the ER, and bypassed the Golgi apparatus via a non-canonical trafficking pathway. In addition, Vx3 was modified to allow inducible release of bound K63-polyUb. By disabling Vx3, tracking of the ubiquitinated proteins to observe their downstream activities becomes possible. This thesis preliminarily identifies K63-polyUb as a signal for what is possibly a quality control pathway and offers tools for further investigation in context of Vx3.

## TABLE OF CONTENTS

ABSTRACT.....	ii
LIST OF TABLES.....	vi
LIST OF FIGURES.....	vii
Chapter 1: Introduction.....	1
1.1 Ubiquitin overview.....	1
1.2 Vx3 as a K63-polyUb sensor.....	1
1.3 Vx3 foci are intracellular K63-polyUb structures.....	2
1.4 Vx3 intersects with autophagy.....	2
1.5 ATG9A co-localizes with Vx3 foci.....	4
1.6 Vx3 foci localize at an ER-endolysosome interface.....	6
Chapter 2: Identification and biochemical characterization of Vx3-associated proteins.....	8
2.1 Introduction.....	8
2.2 Vx3 binds K63-polyubiquitinated transmembrane proteins.....	8
2.3 VMP1 overexpression enriches for Vx3-associated proteins.....	10
2.4 Vx3 co-localizes with TfR and MHC-I.....	12
2.5 ATG9A knockdown mislocalizes TfR and MHC-I.....	12
2.6 Vx3-bound proteins do not originate from endocytosis.....	14
2.7 TfR is K63-polyubiquitinated and unconventionally trafficked.....	14
2.8 Quality control, plasma membrane, trafficking, and caveolae proteins are associated with Vx3.....	17
2.9 Discussion.....	17

2.10 Materials and methods.....	24
2.10.1 Plasmids and antibodies.....	24
2.10.2 Cell culture, transfection, and knockdown.....	24
2.10.3 Co-immunoprecipitation.....	25
2.10.4 Mass spectrometry sample preparation.....	26
2.10.5 Biochemical assays.....	27
2.10.6 Gel electrophoresis and immunoblotting.....	28
2.10.7 Internalization assays.....	28
2.10.8 Immunostaining and microscopy.....	28
Chapter 3: Disabling Vx3.....	30
3.1 Introduction.....	30
3.2 Chemically-induced dimerization.....	30
3.3 Adapting FKBP12-rapamycin-FRB for Vx3.....	31
3.4 FRB-Vx3 is partially disabled in vitro by UbK0-FKBP12 and rapamycin.....	33
3.5 2UbK0-FKBP12 and rapamycin disables FRB-Vx3 in vitro.....	35
3.6 FRB-Vx3 binds endogenous K63-polyUb in mammalian cells.....	37
3.7 2UbK0-FKBP12 forms K63-polyUb-positive aggregates.....	37
3.8 Alternative CID systems.....	39
3.9 A degradation system to modulate protein levels.....	39
3.10 Adapting DD for Vx3.....	39
3.11 Labeling of HaloTagged proteins at DD-Vx3 foci.....	40
3.12 Dynamics at Vx3 foci.....	42
3.13 Discussion.....	42

3.14 Materials and methods.....	43
3.14.1 Plasmids.....	43
3.14.2 Protein expression and purification.....	44
3.14.3 Fluorescence polarization binding assays.....	44
3.14.4 Cell culture.....	45
3.14.5 Fluorescence microscopy.....	45
Chapter 4: Conclusions.....	47
Bibliography.....	50
Appendix 1: Endogenously-tag ATG9A by CRISPR.....	55
A1.1 Introduction.....	55
A1.2 Materials and methods.....	55
A1.2.1 CRISPR/Cas9-mediated genome editing.....	55
A1.2.2 Microscopy.....	56
Appendix 2: Rapamycin system constructs.....	58
List of abbreviations.....	59

## LIST OF TABLES

### Chapter 2

2.1: Vx3-associated proteins identified from LC-MS/MS.....	11
2.2: Vx3-associated proteins identified from the second round of LC-MS/MS.....	19

## LIST OF FIGURES

### Chapter 1

- 1.1 Vx3 foci are K63-polyUb structures that conditionally overlap with autophagic vesicles .....3
- 1.2 Vx3 foci co-localize with and are dependent on ATG9A.....5
- 1.3 Vx3 foci localize to an ER-late endosome or lysosome interface.....7

### Chapter 2

- 2.1 Vx3 co-IP sample preparation for LC-MS/MS .....9
- 2.2 MHC-I and TfR co-localize with Vx3 foci.....13
- 2.3 Vx3-bound proteins do not originate from an endocytic pathway.....15
- 2.4 TfR is K63-polyubiquitinated and unconventionally trafficked.....16
- 2.5 Second Vx3 co-IP sample preparation for LC-MS/MS .....18

### Chapter 3

- 3.1 Schematic of the FKBP12-rapamycin-FRB CID system adapted for Vx3.....32
- 3.2 FRB-Vx3 has high affinity for K63-polyUb.....34
- 3.3 2UbK0-FKBP12 and rapamycin can disable FRB-Vx3.....36
- 3.4 FRB-Vx3 binds endogenous K63-polyUb, but FKBP12 localizes into K63-polyUb-positive foci.....38
- 3.5 ATG9A and TfR accumulate at DD-Vx3 foci on different time-scales.....41

### Appendix 1

- A1.1 Endogenously-tagged ATG9A in Vx3-EGFP cells.....57

### Appendix 2

A2.1 Vx3 rapamycin system constructs.....58

## CHAPTER 1: INTRODUCTION

### 1.1 Ubiquitin overview

Ubiquitin (Ub) is an 8.5 kDa protein that serves as a post-translational modification and plays important roles in numerous cellular processes.<sup>1</sup> Through a cascade of Ub-activating enzyme (E1), Ub-conjugating enzyme (E2), and Ub ligase (E3) reactions, Ub is conjugated to other proteins as a monomer or a polymer. Diverse polyUb chain formations are possible as one Ub's C-terminus can be linked to another Ub at one of its seven lysine residues or the N-terminal amine via an (iso)peptide bond. The "Ub code" has been proposed in which each polyUb linkage confers unique architecture and can specify different signaling pathways.<sup>1</sup> Different linkage types typically mediate multiple functions. Proteins modified by lysine 63-linked polyUb (K63-polyUb), the topic of this study, have been implicated in inflammatory response, DNA repair, endocytosis, and autophagy.<sup>1-4</sup>

### 1.2 Vx3 as a K63-polyUb sensor

Genetically encoded sensors are useful tools for probing specific proteins in vivo. Taking advantage of the unique structures conferred by each polyUb linkage, a sensor that specifically recognizes K63-polyUb was created. Vx3 is a K63-polyUb sensor that consists of three tandem ubiquitin interacting motifs (UIMs) taken from vacuolar protein sorting-associated protein 27 (Vps27). The three UIMs are connected through seven-amino acid alpha helical linkers which orient the UIMs favorably to bind K63-polyUb over other linkages. Through avidity effects, Vx3 has a high affinity for its target, with  $K_d = 7.4$  nM for K63-triUb, and thereby acts as a competitive inhibitor for endogenous K63-polyUb receptor proteins.<sup>5</sup> Binding partners are unable to interact with Vx3-bound K63-polyUb and downstream signaling is blocked. Vx3 is a

useful probe for identifying K63-polyubiquitinated proteins and studying the purpose of K63-polyUb signals.

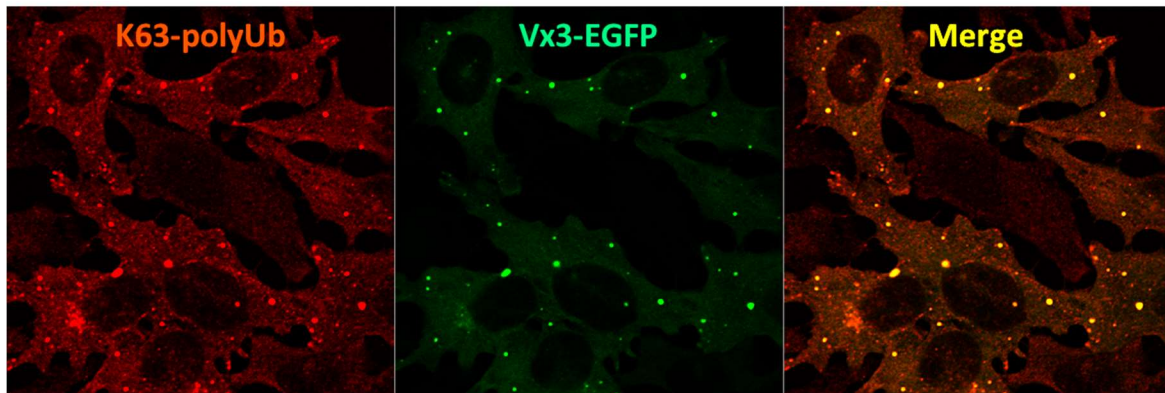
### **1.3 Vx3 foci are intracellular K63-polyUb structures**

When expressed in cells, Vx3 forms cytoplasmic foci. This phenotype is absent when expressing a non-binding version of Vx3 (Vx3NB) where the UIMs are mutated and unable to bind Ub. Vx3NB remains diffused throughout the cell.<sup>5</sup> Vx3 expression has elicited foci when expressed in all cell lines tested: HeLa (human cervical cancer cells), U2OS (cancerous human bone cells), COS-7 (immortalized fibroblast-like cells from African green monkey kidney), HEK293T (human embryonic kidney with mutant SV40 large T antigen), RAW (mouse macrophages), MEF (mouse embryonic fibroblasts), and H9c2(2-1) (rat myoblasts). The formation of foci suggests that when Vx3 binds K63-polyUb, the sensor accumulates ubiquitinated proteins in the cytoplasm. However, this phenotype doesn't account for all intracellular K63-polyUb, because Vx3 foci do not co-localize with all K63-polyUb structures (FIG 1.1.A). Thus, these Vx3 foci are the result of a specific subset of K63-polyubiquitinated proteins.

### **1.4 Vx3 intersects with autophagy**

Autophagy, sometimes referred to as “macroautophagy,” is a mechanism that targets select cytosolic components, which can range from individual proteins to intact organelles and invading pathogens, to be sequestered into double-membrane vesicles termed autophagosomes. These specialized vesicles then fuse with lysosomes to degrade and recycle the targeted components.<sup>6</sup> A subset of Vx3 foci were previously shown to co-localize with the autophagy marker microtubule-associated protein 1A/1B-light chain 3 (LC3), which in its lipidated form is embedded in autophagosome membranes.<sup>5</sup> However, further experiments show that in cells

A



B

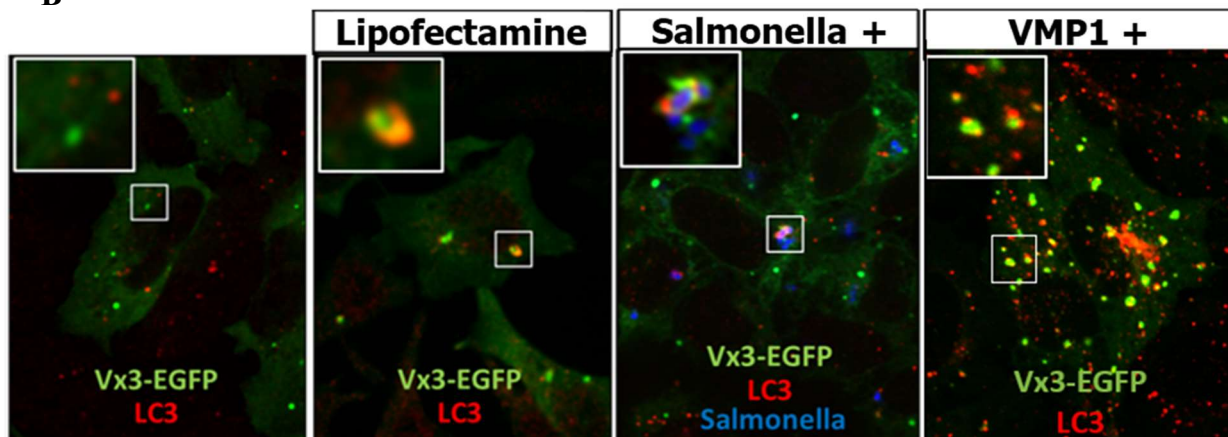


**FIG 1.1 Vx3 foci are K63-polyUb structures that conditionally overlap with autophagic vesicles.** (A) HeLa cells transfected with Vx3-EGFP were immunostained with an anti-K63-polyUb antibody. (B) HeLa cells stably expressing Vx3-EGFP under the control of a Dox-inducible promoter were induced with 1  $\mu\text{g}/\text{mL}$  Dox for 24 h and were treated with Lipofectamine 2000, infected with *Salmonella* Typhimurium, or transfected with a plasmid encoding VMP1. Cells were stained with an anti-LC3 antibody. Vx3 signals co-localize with autophagy marker LC3 only upon treatments for autophagy induction. All experiments were performed by Francesco Scavone.

stably expressing Vx3, LC3 does not co-localize with Vx3 foci without selective autophagy stimuli (FIG 1.1.B). Adding cationic lipids such as transfection reagent Lipofectamine 2000 induces co-localization of Vx3 with autophagic vesicles. The same result is also seen when cells are infected with *Salmonella* Typhimurium and undergo selective autophagy as a defense mechanism against invading bacteria. Interestingly, overexpressing vacuole membrane protein 1 (VMP1), an ER-resident membrane protein involved with autophagosome biogenesis, results in increased Vx3/LC3 co-localization as well as more robust Vx3 foci. While Vx3 foci don't co-localize with LC3 in the absence of selective autophagy induction, it's possible that the proteins trapped in Vx3 foci are still related to autophagy pathways. If Vx3 inhibits autophagy during early autophagosome biogenesis, LC3 isn't present, and a lack of LC3 co-localization would be a false negative for autophagic activity. However, it is also possible that the K63-polyubiquitinated proteins were undergoing pathways unrelated to autophagy before being inhibited by Vx3.

### **1.5 ATG9A co-localizes with Vx3 foci**

While Vx3 foci may not always co-localize with the conventional autophagy marker LC3, they co-localize well with autophagy-related protein 9 (ATG9A) (FIG 1.2.A). Moreover, all Vx3 foci are lost upon ATG9A knockdown (FIG 1.2.B). ATG9A is the only transmembrane protein known to be required for autophagy.<sup>7</sup> It traffics extensively throughout the cell between the Golgi apparatus, plasma membrane, and recycling endosomes, and it has been speculated that ATG9A vesicles carry membranes from these different organelles as a source of lipids to build autophagosomes during autophagy.<sup>8,9</sup> However, ATG9A's function is largely unknown. Studying Vx3 foci may reveal more about ATG9A's role in the cell.

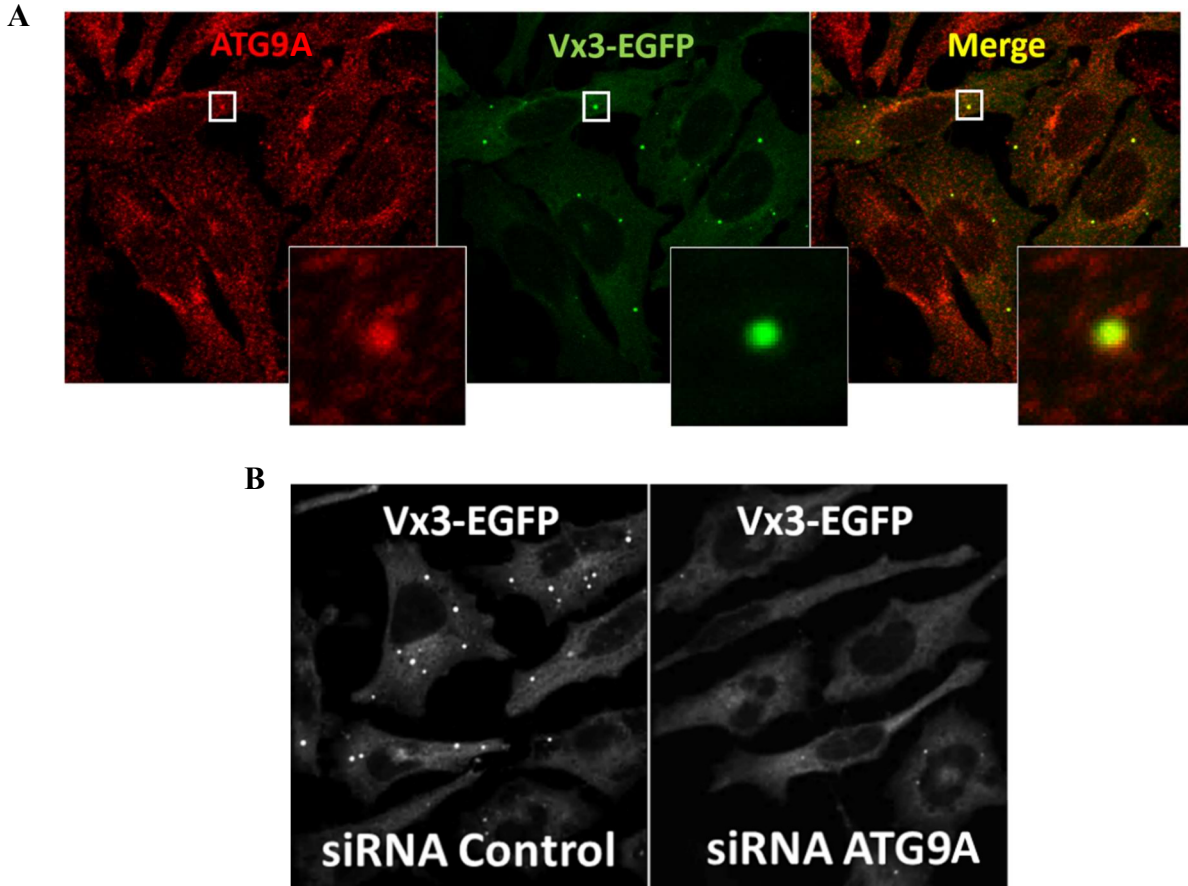


**FIG 1.2 Vx3 foci co-localize with and are dependent on ATG9A.** (A) HeLa cells stably expressing Vx3-EGFP were stained with an anti-ATG9A antibody. (B) Vx3-EGFP stable cells were transfected with either control siRNA or siRNA against ATG9A for 72 h. Vx3-EGFP expression was induced in the last 24 h by treatment with 1  $\mu$ g/mL Dox. These experiments were performed by Francesco Scavone.

## 1.6 Vx3 foci localize at an ER-endolysosome interface

Cytosolic Vx3 foci consistently co-localize with various endosome and lysosome markers (FIG 1.3.A, B). Ras-related protein Rab-7A (Rab7a) marks late endosomes, and both lysosomal associated membrane protein 1 (LAMP1) and CD63 are considered late endosomal and lysosomal markers. These proteins do not identify a specific organelle, so Vx3 could be co-localizing with late endosomes, endolysosomes, or lysosomes. Also, it isn't clear whether Vx3 foci are inside or just nearby late endosomes/lysosomes. Overexpression of the GTPase-defective mutant Rab5Q79L-mCherry enhances fusion of endosomes.<sup>10</sup> The resulting enlarged endosomes provides enough spatial resolution to show that Vx3 foci localize to the edge of Rab5Q79L-positive endosomes at a stage where ER membranes are contacting both the endosomes and Vx3 foci (FIG 1.3.C).

These results show that Vx3 foci co-localize with ATG9A, and foci formation is dependent on ATG9A. Vx3 foci also localize to an ER-endolysosome interface. Given that Vx3 foci co-localize with LC3 upon autophagy induction, autophagic vesicles may converge with the K63-polyubiquitinated proteins targeted by Vx3 at a stage prior to fusion with lysosomes. It's also possible that the ubiquitinated proteins are related to or undergoing autophagy themselves. There are many questions that remain, including the identity of the K63-polyubiquitinated proteins, the function of the K63-polyUb signal, the Ub conjugating enzymes responsible, and the involvement of downstream K63-polyUb receptor proteins. The research in the following chapters provides further insight about the ubiquitinated proteins associated with Vx3 and offers new tools for probing K63-polyUb-dependent processes and trafficking of K63-polyubiquitinated proteins.

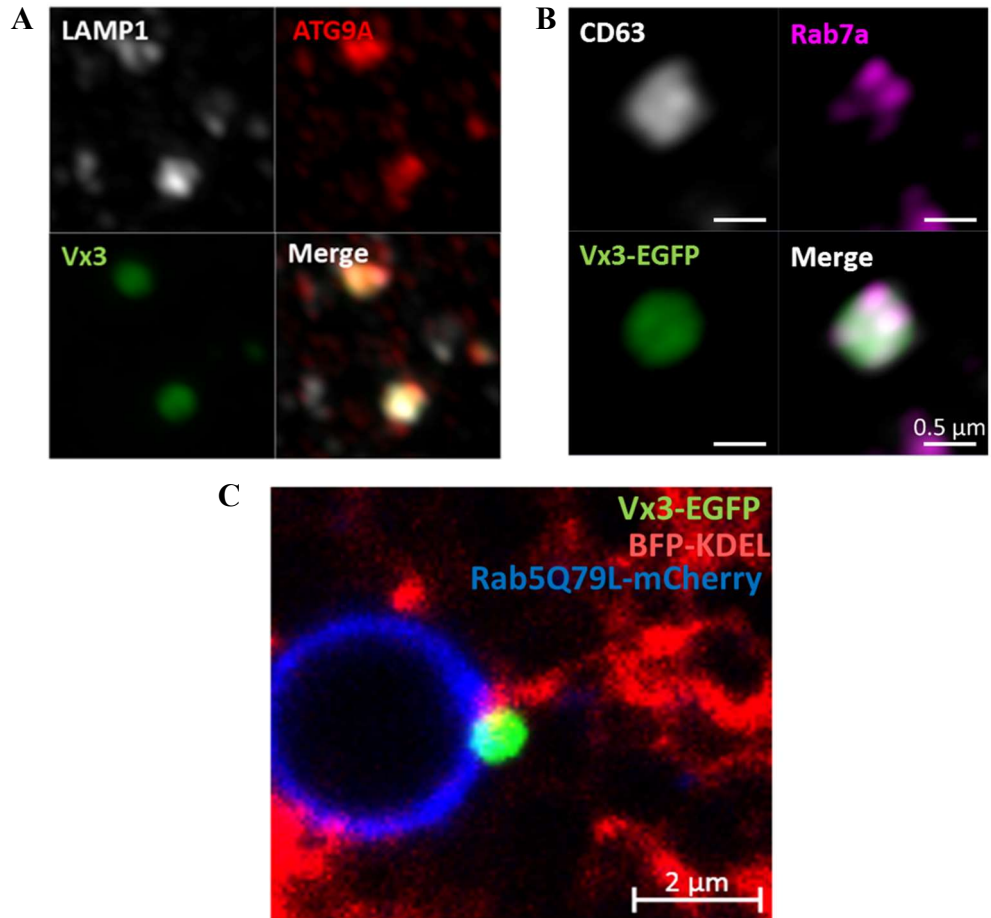


**FIG 1.3 Vx3 foci localize to an ER-late endosome or lysosome interface.** HeLa cells stably expressing Vx3-EGFP were stained with antibodies for (A) ATG9A and late endosomal/lysosomal marker LAMP1 or (B) late endosomal marker Rab7a and late endosomal/lysosomal marker CD63. (C) Cells stably expressing Vx3-EGFP were co-transfected with ER marker BFP-KDEL and Rab5Q79L-mCherry which forms large endosomes. All images were taken using Airyscan superresolution. These experiments were performed by Francesco Scavone.

## CHAPTER 2: IDENTIFICATION AND BIOCHEMICAL CHARACTERIZATION OF Vx3-ASSOCIATED PROTEINS

### **2.1 Introduction**

Previous studies from our lab have shown that Vx3 foci are ATG9A dependent, localize to ER-endolysosome interfaces, and co-localize with LC3 upon selective autophagy induction. To further understand the nature of Vx3 foci, the K63-polyubiquitinated proteins were identified by coupling co-immunoprecipitation (co-IP) and mass spectrometry, a common method for identifying protein-protein interactions. This chapter details the identification of ubiquitinated proteins directly bound by Vx3 as well as associated proteins. Preliminary characterization of the identified proteins show that a population of transmembrane proteins are unconventionally trafficked from the ER, possibly representing a new quality control pathway.

### **2.2 Vx3 binds K63-polyubiquitinated transmembrane proteins**

Three different HeLa stable cell lines were analyzed: 1) 3xFLAG-Vx3NB-EGFP as a control to identify proteins that may nonspecifically interact with the sensor in the absence of K63-polyUb, 2) 3xFLAG-Vx3-EGFP, and 3) co-expression of Vx3-EGFP and VMP1-HA-iRFP to determine whether autophagy induction through VMP1 overexpression causes additional proteins to be ubiquitinated or associated with Vx3. The co-IPs were performed under partially denaturing conditions to preserve Vx3 and K63-polyUb binding while minimizing nonspecific interactions. After co-IP with an anti-GFP nanobody, two sequential elutions separated the sensors from the rest of the co-IP samples; Vx3 associated proteins were enriched in the primary elution at room temperature while Vx3 and Vx3NB were only eluted upon boiling (FIG 2.1.A). The elutions were then further fractionated by gel extraction (FIG 2.1.B), trypsinized, and

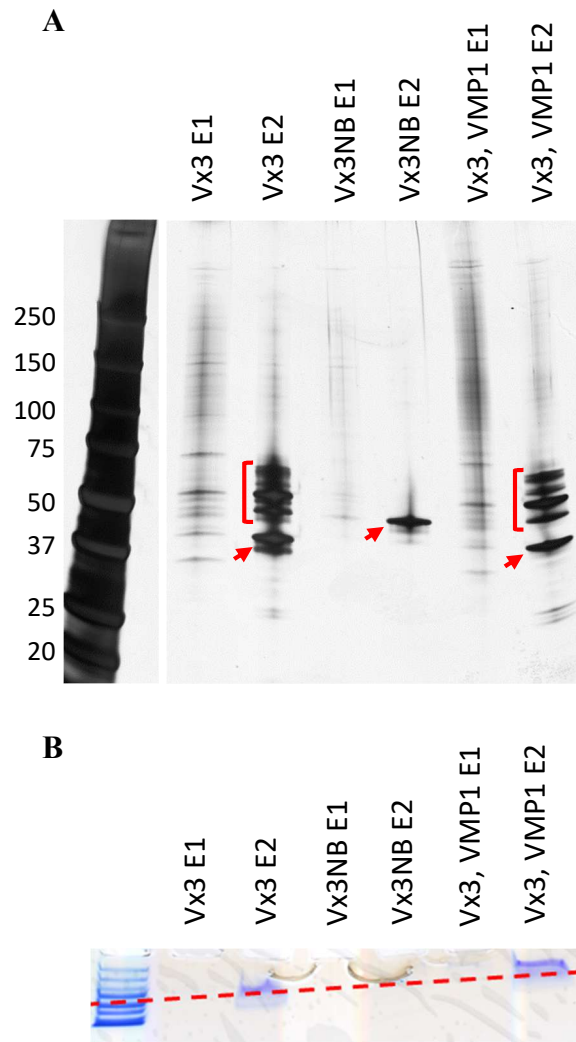


**FIG 2.1 Vx3 co-IP sample preparation for LC-MS/MS.** HeLa cells stably expressing Vx3NB-EGFP, Vx3-EGFP, or Vx3-EGFP with VMP1-iRFP after 48 h of 1  $\mu$ g/mL Dox were co-IPed for Vx3. The first elution was performed at room temperature, and the second one was performed at 70°C. (A) The SDS-PAGE gel visualized by silver staining shows that the sensor was separated into the second elution. The red arrows indicate Vx3 or Vx3NB, and the brackets indicate ubiquitinated Vx3. (B) In order to fractionate the samples further for LC-MS/MS, the elutions in the Coomassie-stained gel were extracted as <70 kDa and >70 kDa by cutting the gel along the red dashed line.

analyzed by tandem liquid chromatography-mass spectrometry (LC-MS/MS). The identified proteins are potentially ubiquitinated and bound to Vx3-EGFP, but they could also be proteins associated with the ubiquitinated proteins. Trypsin cleaves polypeptides at the carboxyl side of lysine and arginine. When Ub is digested, a Gly–Gly (GG) peptide is the most C-terminal fragment. If a protein is ubiquitinated, the lysine where Ub is conjugated carries a GG Ub remnant that adds 114.043 Da to the tryptic peptide; this allows accurate identification of ubiquitinated proteins.<sup>11</sup> Focusing on proteins with GG remnants helped narrow the mass spectrometry results to ubiquitinated proteins.

Interestingly, proteomics analysis for peptides that were enriched in Vx3 co-IPed samples (i.e., peptides with higher unique spectral counts compared to Vx3NB co-IPed samples) showed that the most prominent hits were transmembrane proteins known to localize at the plasma membrane and be involved in endocytic trafficking (TABLE 2.1). These transmembrane proteins include transferrin-receptor (TfR), major histocompatibility complex class I (MHC-I), integrin- $\beta$ 1 (ITGB1), and caveolin-1 (CAV1). There were no ATG9A peptides. The lysis conditions for co-IP solubilized all membranes, so ATG9A vesicles are in solution as well. The lack of peptides associated with Vx3 indicates that ATG9A doesn't directly interact with Vx3. Consistently, we have not been able to observe ATG9A ubiquitination (data not shown).

### **2.3 VMP1 overexpression enriches for Vx3-associated proteins**

Although there weren't any new proteins identified from HeLa cells co-expressing 3xFLAG-Vx3-EGFP and VMP1-HA-iRFP, the IP sample from these cells exhibited a higher number of unique spectral counts for many of the identified transmembrane proteins. This is consistent with the enriched cytosolic Vx3-EGFP foci observed by VMP1 overexpression. VMP1 peptides were only identified in immunoprecipitates from VMP1-iRFP expressing cells,

**TABLE 2.1 Vx3-associated proteins identified from LC-MS/MS.** Lysates from HeLa cells stably expressing Vx3NB-EGFP non-binding control, Vx3-EGFP, or Vx3-EGFP with VMP1-iRFP were immunoprecipitated with GFP Trap nanobodies. The captured proteins were digested with trypsin and subjected to LC-MS/MS. A selection of the identified proteins is shown with corresponding peptide counts from the analysis. These proteins are potentially modified by K63-polyUb and localized to Vx3 foci.

Gene Name	Human Gene Descriptions	Total Peptide Count		
		Stable Cell Line		
		Vx3NB	Vx3	Vx3, VMP1
ATG9A	Autophagy-related protein 9A	-	-	-
VMP1	Vacuole membrane protein 1	-	-	6
TFRC	Transferrin receptor (TfR)	-	11	32
HLA-A	MHC class I A-69 alpha chain (MHC-I)	-	6	11
MIF	Macrophage migration inhibitory factor	7	22	28
ITB1	Integrin beta-1 (ITGB1)	-	2	5
SQSTM1	Sequestosome-1; p62	-	4	25
CAV1	Caveolin-1	-	2	1
HUWE1	E3 ubiquitin-protein ligase HUWE1	-	3	7
IGF2R	Cation-independent mannose-6-phosphate receptor	-	-	3

meaning that overexpressed but not endogenous VMP1 is detectably modified by K63-polyUb and bound by Vx3 (TABLE 2.1).

#### **2.4 Vx3 co-localizes with TfR and MHC-I**

The ubiquitinated transmembrane proteins are potential candidates for studying Vx3 foci. To determine which one would be best suited as a model K63-polyubiquitinated protein bound by Vx3, cells stably expressing Vx3-EGFP were immunostained for endogenous TfR and MHC-I. Both proteins co-localized well with Vx3 foci (FIG 2.2.A). However, the vast majority of intracellular TfR and MHC-I in the cytosol didn't co-localize with Vx3, which suggests that only a small subset of these two transmembrane proteins were modified by K63-polyUb. Both TfR and MHC-I are appropriate targets for studying Vx3 based on their readily detectable endogenous populations at Vx3 foci.

#### **2.5 ATG9A knockdown mislocalizes TfR and MHC-I**

ATG9A plays an important role in Vx3-EGFP foci formation, because no Vx3 foci form after ATG9A knockdown. Surprisingly, knockdown of ATG9A also reduced intracellular staining of TfR and MHC-I in HeLa cells (FIG 2.2.B). TfR and MHC-I have been reported to reside within the recycling endosomal system. They are located on the plasma membrane, but after endocytosis, they typically reach early endosomes before trafficking to recycling endosomes and subsequently returning to the cell surface.<sup>12,13</sup> This data suggests that ATG9A may play a role in the sorting of TfR and MHC-I to the recycling pathway. Knockdown of ATG9A may result in missorting and delivery of these transmembrane proteins to lysosomes for degradation. This function of ATG9A is previously unknown and independent of autophagy. Future experiments are needed to firmly establish this new function.

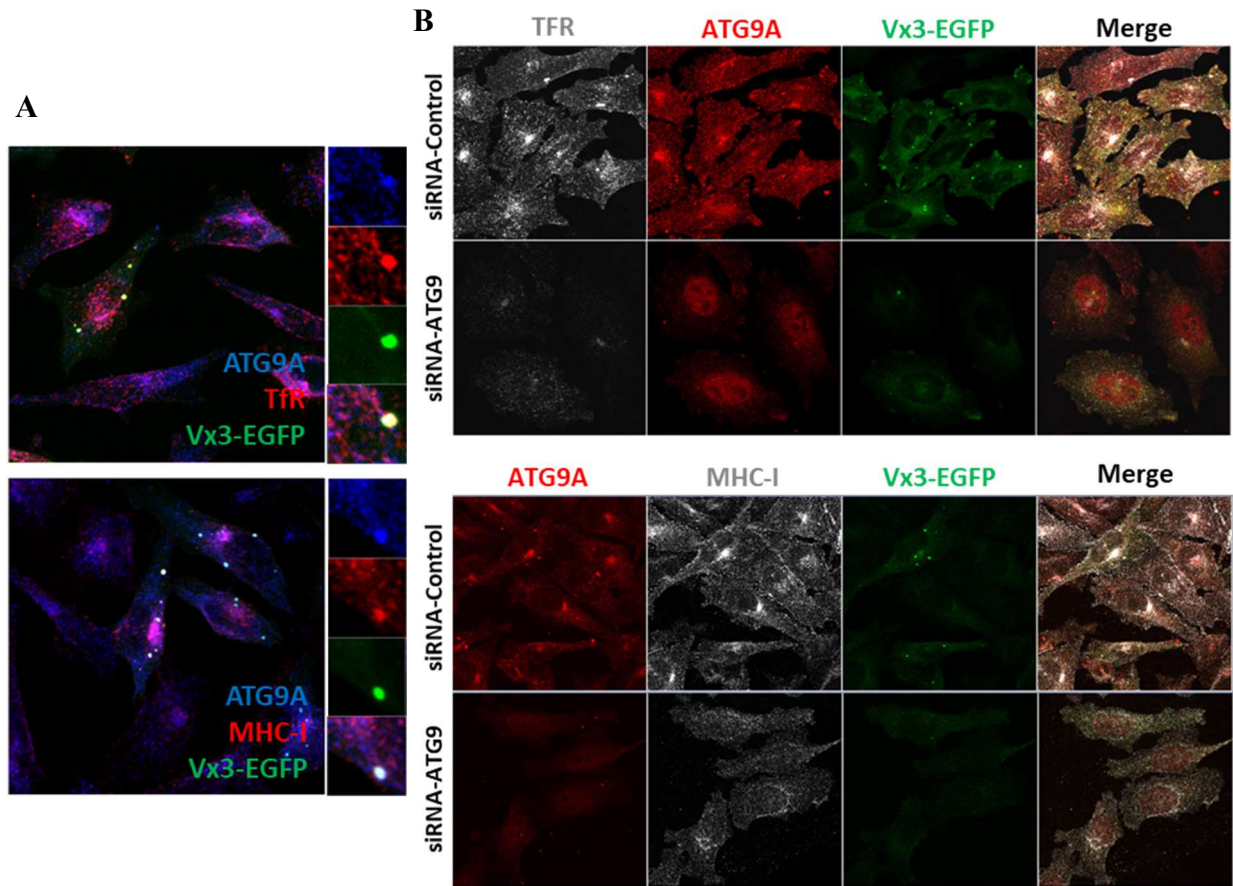


**FIG 2.2 MHC-I and TfR co-localize with Vx3 foci.** (A) Vx3-EGFP stable cells were stained for endogenous ATG9A, TfR, and MHC-I. This experiment was performed by Francesco Scavone. (B) HeLa cells stably expressing Vx3-EGFP were transfected with ATG9A siRNA for 72 h. Vx3-EGFP expression was induced for the last 24 h with 1  $\mu$ g/mL Dox. The cells were stained using anti-ATG9A and anti-TfR or anti-MHC-I antibodies.

## **2.6 Vx3-bound proteins do not originate from endocytosis**

To determine whether the transmembrane proteins that associate with Vx3 are of endocytic origin, cells were immunostained with antibodies for early endosome antigen 1 (EEA1) and Ras-related protein Rab-11A (Rab11A), markers for endocytic recycling.<sup>12</sup> Vx3 didn't co-localize with these endocytic recycling markers (FIG 2.3.A, B). Internalization assays were also performed to complement these results. MHC-I antibodies and fluorescently-labeled transferrin, the ligand for TfR, were added to cells. Internalized Tf-640 and MHC-I antibody didn't co-localize with Vx3 (FIG 2.3.C, D). These results suggest that the K63-polyubiquitinated proteins in Vx3 foci did not originate from the plasma membrane through endocytosis.

## **2.7 TfR is K63-polyubiquitinated and unconventionally trafficked**

Vx3 is a highly specific K63-polyUb sensor *in vitro*.<sup>5</sup> To identify the Ub-Ub linkage type involved in Vx3 binding in cells, Vx3-EGFP co-IPed samples were digested with a variety of deubiquitinating enzymes (DUBs). The panel of DUBs consisted of OTUB1 (K48-Ub specific), AMSH (K63-Ub specific), and USP2c (catalytic core of a pan-specific DUB).<sup>14</sup> Most proteins eluted after co-IP with Vx3 appear as a high molecular-weight smear due to polyubiquitin modifications. Upon hydrolysis by DUBs, the smear should resolve as a band at the protein's expected size. TfR is a bona fide K63-polyubiquitinated cargo (FIG 2.4). In cells, functional TfR exists as a dimer at the cell surface visible by SDS-PAGE,<sup>12</sup> but only the monomeric form of TfR was pulled down with Vx3. One possibility is that only TfR monomers that are unassembled or misfolded are modified by K63-polyUb and targeted for Ub-dependent protein quality control.

To complement the microscopy-based experiments which showed that ubiquitinated proteins don't originate from the plasma membrane, an additional biochemical test was

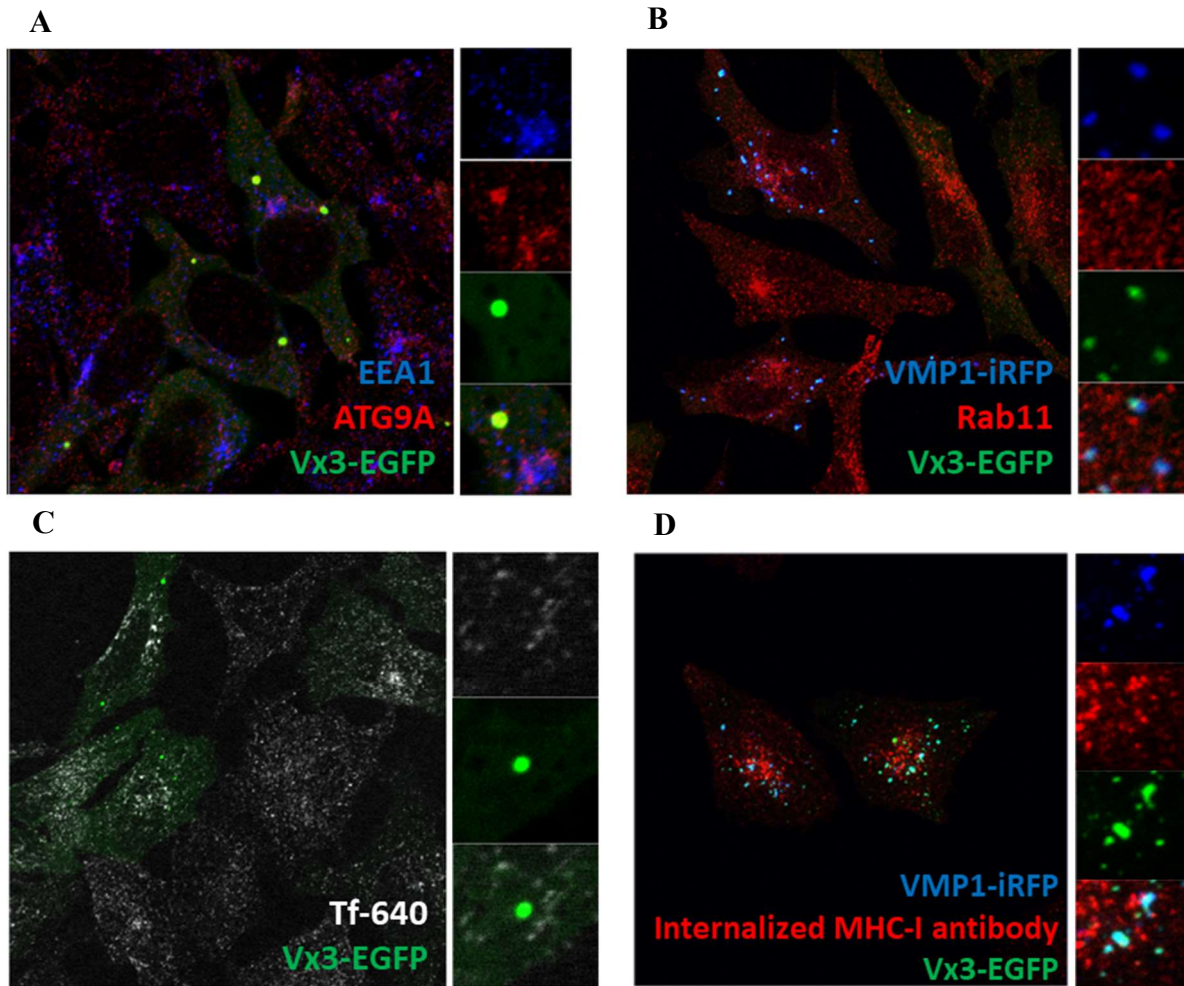


**FIG 2.3 Vx3-bound proteins do not originate from an endocytic pathway.** (A) HeLa cells stably expressing Vx3-EGFP were stained using anti-EEA1 and anti-ATG9A antibodies. (B) HeLa cells stably expressing Vx3-EGFP and VMP1-iRFP were stained for recycling endosome marker Rab11. (C) Vx3-EGFP stable cells were incubated with Tf-640 for 2 h. Endocytosed Tf-640 didn't co-localize with Vx3-EGFP. (D) Vx3-EGFP and VMP1-iRFP stable cells were incubated with anti-MHC-I antibodies for 1 h. Vx3 foci didn't co-localize with internalized MHC-I. All experiments were performed by Francesco Scavone.

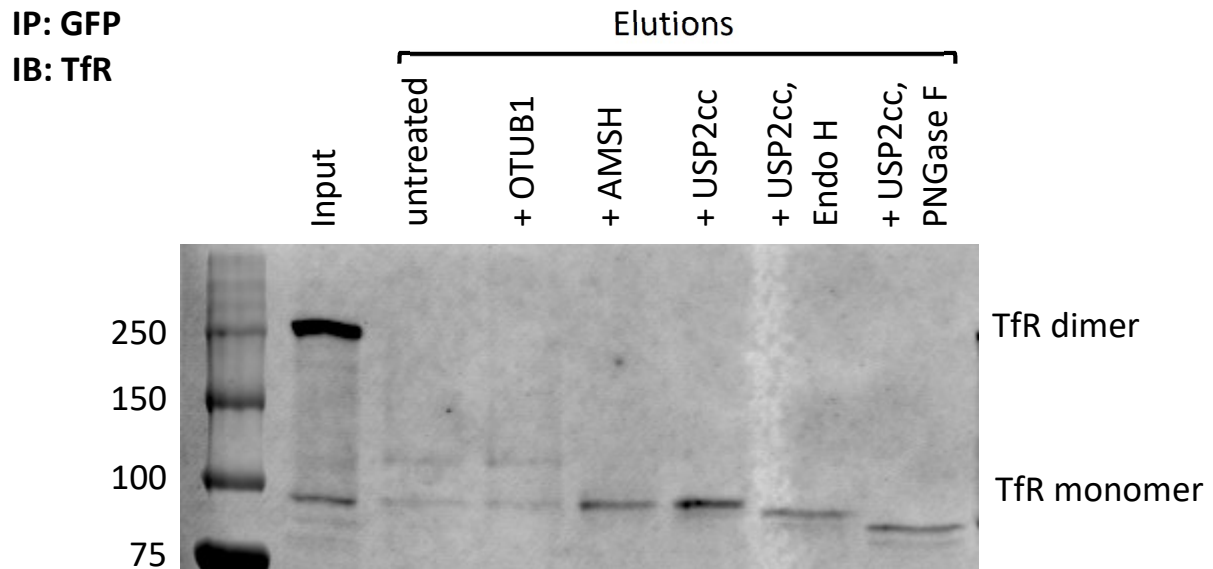


**FIG 2.4 TfR is K63-polyubiquitinated and unconventionally trafficked.** Cells stably expressing 3xFLAG-Vx3-EGFP were immunoprecipitated with a GFP nanobody. The co-IP samples were then subjected to linkage-specific and pan-specific DUBs. Ubiquitinated TfR is sensitive to the K63-Ub specific DUB, AMSH. Samples digested with the pan-specific DUB, USP2cc, were also subjected to glycosidase digestion. TfR is sensitive to Endo H, a glycosidase that identifies proteins that have been modified at the ER but not the Golgi apparatus.

performed on the co-IP elutions to determine the glycosylation status of the cargo proteins. Endo H is a glycosidase that cleaves high mannose oligosaccharides added to proteins in the ER, but Endo H cannot cleave oligosaccharides that were further modified at Golgi apparatus. PNGase F cleaves all high mannose oligosaccharides, even on proteins that have trafficked to the Golgi.<sup>15</sup> The Vx3-bound TfR is Endo H sensitive; therefore, it did not traffic from the ER to the Golgi following translation (FIG 2.4).

## **2.8 Quality control, plasma membrane, trafficking, and caveolae proteins are associated with Vx3**

The first mass spectrometry experiment (TABLE 2.1) was informative, but a second run was scaled up to provide deeper analysis. The 3xFLAG-Vx3NB-EGFP and 3xFLAG-Vx3-EGFP stable cell conditions remained the same, but a sample of Vx3-EGFP-expressing cells were additionally treated with transfection reagent Lipofectamine 3000 to induce for an autophagy response. For this round of LC-MS/MS, only samples from the primary elution were analyzed (FIG. 2.5). Similar to overexpression of VMP1, autophagy induction did not lead to identification of new Vx3-associated proteins. In the second mass spectrometry experiment, there were thousands of proteins identified, making it difficult to parse through the results. However, by just focusing on the most abundant peptides, the identified proteins can be sorted into the following categories: caveolae, plasma membrane, trafficking, autophagy, quality control, and E3 ligases (TABLE 2.2).

## **2.9 Discussion**

While the first mass spectrometry experiment mainly identified transmembrane proteins localized at the plasma membrane, the second experiment yielded many more proteins that

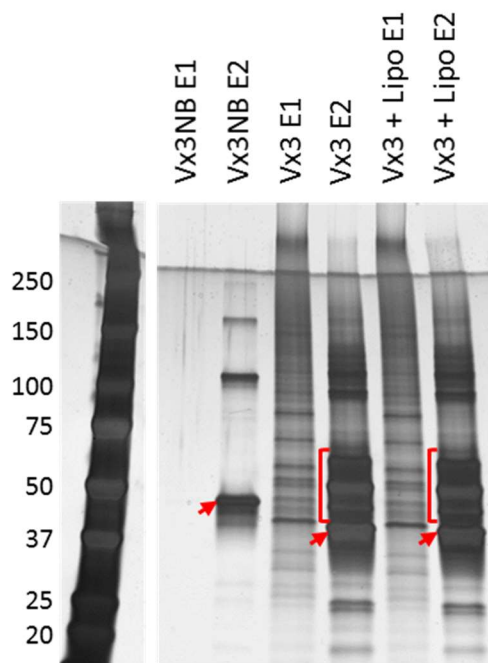


**Figure 2.5 Second Vx3 co-IP sample preparation for LC-MS/MS.** HeLa cells were induced with Dox for 48 h to stably express Vx3NB-EGFP, Vx3-EGFP, or Vx3-EGFP treated with Lipofectamine 3000 in the last 4 h. The elutions from co-IP are visualized in the SDS-PAGE gel by silver staining. Vx3NB or Vx3 are indicated by red arrows, and ubiquitinated Vx3 is indicated by the red brackets.

**TABLE 2.2 Vx3-associated proteins identified from the second round of LC-MS/MS.** A categorized list including proteins from the top 200 hits from GFP co-IP of cells stably expressing 3xFLAG-Vx3-EGFP. Abundance is based on total spectral counts/protein molecular weight (SC/MW). GG peptide number is indicated along with all ubiquitination sites. General protein descriptions were written based on information available in the databases UniProt (<https://www.uniprot.org/>), NCBI (<https://www.ncbi.nlm.nih.gov/>), and GeneCards (<https://www.genecards.org/>). The table was prepared with assistance from Francesco Scavone.

	Gene Name	Abundance (SC/MW)	# GG peptides	Ub site	Description
Caveolae	CAV1	982	19	K5, K26, K30, K39, K47	caveolae biogenesis
	ANKRD13A	370	1	K563	late endosome; binds K63-Ub; CAV1 to lysosome
	CAVIN1	343	4	K98, K161, K276	caveolae biogenesis
	CAV2	153	7	K7	caveolae biogenesis
	FLOT1	129	0		caveolae biogenesis
Plasma Membrane	STOM	391	0		melanosome integral protein
	SLC1A5	327	11	K10, K372, K502, K522, K537	amino acid transporter
	TFRC	299	11	K39, K53	TfR; recycling endosome
	CLIC4	142	1	K60	chloride intracellular channel
	FAT1	133	4	K4325, K4346	pro-cadherin; cell migration
	HLA-A	130	4	K340, K364	MHC-I; antigen cross-presentation
	LY6K	123	0		cell growth
	MARCKSL1	123	2	K110	cell migration
	ITGB1	118	6	K774, K784, K794	cell adhesion
	ITM2B	92	3	K13, K39	neurite outgrowth
	LIMS1	91	0		cell growth

	ATP1B1	88	0		cell adhesion
	ATP1B3	83	0		ion transport
	SLC4A2	80	6	K653, K658	anion transport
Trafficking	RAB7A	477	9	K97, K126, K175, K191, K194	late endosome
	VAMP3	327	11	K35, K42, K66	v-SNARE; recycling endocytic TfR; late endosome to TGN
	ARF3	316	0		GTP-binding; Golgi
	ARF4	273	0		GTP-binding; Golgi
	VAMP7	261	16	K115, K125, K137, K160, K172	v-SNARE; early endosome/autophagosome with lysosome
	VAMP2	190	11	K52, K59, K83	v-SNARE; exocytosis; clathrin-independent endocytosis
	SCAMP3	141	6	K81, K101, K102, K313	post-Golgi recycling
	SCAMP4	109	8	K4, K185	post-Golgi recycling
	SNAP23	116	0		membrane fusion
	MYOF	116	2	K1436, K1805	endocytic recycling, plasma membrane repair, exosomes
	SCAMP1	90	7	K19, K65, K89, K298, K334	post-Golgi recycling
	STX6	82	0		t-SNARE; TGN; endosomes
STX10	78	0		t-SNARE; late endosome to TGN	
Autophagy	SQSTM1	1340	4	K141, K157, K313, K435	p62; selective autophagy cargo receptor
	LAMTOR5	177	0		mTOR complex
	TOMM20	147	0		mitophagy
	FUNDC1	123	2	K119	mitophagy
	DIABLO	133	1	K123	mitophagy
	FUNDC2	111	6	K35, K68, K150	mitophagy
	LAMTOR2	111	0		mTOR complex
	TMEM59	105	4	K315	Golgi; unconventional autophagy
LAMTOR1	85	2	K20	mTOR complex	

Quality Control	HSP90AA2P	452	2	K112, K153	chaperone
	UBQLN2	234	3	K43	ERAD
	UBQLN1	213	3	K47	ERAD
	FAF2	146	0		ERAD
	UBQLN4	144	0		ERAD
	DNAJC5	108	1	K137, K139	chaperone
	BAG6	96	0		ERAD
	UBAC2	92	0		ERAD
	SRP72	88	3	K84, K391, K600	cotranslational protein targeting
	SPCS2	88	0		cotranslational protein targeting
	AUP1	85	0		translocation ER to proteasome
E3 ligases	TRIM25	634	6	K112, K320, K416, K425, K439	K63 for NF- $\kappa$ B signaling
	PJA2	355	6	K268, K304, K320	innate immune response
	MIB1	222	18	K28, K222, K437, K485, K735, K749, K772, K787, K936, K938, K949	Notch signaling; K63 endocytosis
	TRIM26	217	1	K179	innate immune response
	RNF5	191	7	K68, K75	K63 for ERAD; K48 by virus
	HUWE1	156	0		K48 on K63 for NF- $\kappa$ B signaling, for proteasome
	ITCH	153	4	K432, K478	K63 seed in K48/K63 for proteasome
	STUB1	120	0		K48 for proteasome; K27 for NF- $\kappa$ B signaling
	KCMF1	117	0		neutrophil degranulation
	DZIP3	105	5	K212, K1066, K1087	proteasome degradation
	PJA1	89	1	K399	protein sorting
	ZNRF1	84	0		neuronal cell differentiation; K48
	CUL1	83	0		cell cycle progression
SMURF1	81	0		proteasome degradation	

regulate different processes. Not every protein identified can be assumed to directly interact with Vx3. The semi-denaturing co-IP conditions in principle solubilize all membranes, but proteins tightly associated with polyubiquitinated Vx3-bound proteins are also present in the samples as well. Furthermore, there is diffused Vx3 in the cytoplasm; the identified proteins include those associated with the diffused population of Vx3 as well as the proteins associated with Vx3 foci. Integral transmembrane proteins were identified again, but there were also more caveolae-associated proteins. Caveolae are specialized lipid rafts that form invaginations in the plasma membrane, and caveolins are the primary integral membrane components. The canonical form of endocytosis is clathrin-mediated, but a prominent form of clathrin-independent endocytosis occurs via caveolae.<sup>16,17</sup> Other trafficking-related proteins included SNAREs implicated in vesicle fusion with the plasma membrane, such as vesicle-associated membrane protein 3 (VAMP3) and vesicle-associated membrane protein 7 (VAMP7).<sup>18</sup> Identification of these proteins associated with Vx3 suggests that the ubiquitinated transmembrane proteins are possibly en route to the plasma membrane. However, it's also possible that some of the ubiquitinated proteins this thesis didn't focus on originated from endocytosis via caveolae.

The presence of autophagy related proteins, even in the absence of selective autophagy induction, supports the idea that the ubiquitinated proteins are fated for or related to autophagy processes. Also, the lack of co-localization with autophagosome marker LC3 suggests that Vx3 inhibited these proteins from proceeding with autophagy early on in the pathway before autophagosome biogenesis completion.

In addition to transmembrane proteins, the second round of mass spectrometry also identified proteins implicated in quality control mechanisms, mainly ER-associated degradation (ERAD) which encompasses a slew of pathways that target newly synthesized misfolded

proteins for proteasomal degradation.<sup>19</sup> However, there are ERAD-resistant misfolded proteins such as mutant forms of gonadotropin-releasing hormone receptor (GnRHR),  $\alpha$ 1-antitrypsin Z (ATZ), and procollagen that undergo other forms of quality control which target them to lysosomes for degradation.<sup>20-23</sup> Of the identified proteins, heat shock protein 90 (HSP90) is one of the major eukaryotic chaperones, and DnaJ homolog subfamily C member 5 (DNAJC5) is a co-chaperone with HSP70 (which had no peptides identified). DNAJC5 is implicated in an unusual misfolding-associated protein secretion (MAPS) pathway where a subset of misfolded cytosolic proteins is sent to non-degradative lysosomes for secretion from the cell.<sup>24,25</sup>

There were many peptides from E3 Ub ligases. They are highly enriched and not all of the ligases are known for making K63-polyUb. Without further experiments, it's difficult to speculate if any of them are responsible for ligating K63-polyUb onto the transmembrane proteins bound by Vx3.

Comparing the two LC-MS/MS experiments, there were many more macrophage migration inhibitory factor (MIF) peptides in the first experiment. This might be attributed to the cell line stably co-expressing 3xFLAG-Vx3-EGFP and VMP1-HA-iRFP being mildly contaminated with mycoplasma (just barely detectable by PCR, data not shown). MIF is a cytoplasmic cytokine that plays a role in immune response, and mycoplasma contamination may have upregulated the population of MIF that was trapped by Vx3. All cell lines were mycoplasma-free for the second LC-MS/MS experiment.

All results thus far support the possibility that the newly synthesized transmembrane proteins detected by LC-MS/MS are undergoing a quality control pathway terminating either in degradation or unconventional secretion to the plasma membrane. Vx3 was found to be associated with many plasma membrane proteins, quality control proteins, and proteins that

mediate vesicle fusion. K63-polyUb signaling is important for targeting to or fusion with lysosomes, because Vx3 accumulates these ubiquitinated proteins into foci at an ER-endolysosome interface. In the context of selective autophagy induction, Vx3 may stall autophagic vesicles at a stage prior to lysosome fusion as well.

## **2.10 Materials and methods**

### *2.10.1 Plasmids and antibodies*

Francesco Scavone cloned the plasmids used for stable cell line generation. Vx3NB and Vx3 in pEGFP plasmids<sup>5</sup> were subcloned into pcDNA5/FRT/TO plasmids with a N-terminal 3xFLAG tag. VMP1 was subcloned from pMRXIP-hVMP1-GFP (a gift from Noboru Mizushima, The University of Tokyo) into the retroviral vector pQCXIP with a C-terminal HA-iRFP682 tag. The original iRFP682 plasmid was a gift from Vladislav Verkhusha (Addgene #45459; Albert Einstein College of Medicine).

The following antibodies were purchased: anti-ATG9A (rb, 108338, Abcam), anti-MHC-I (ms, 66013-1-Ig, Proteintech), anti-TfR (ms, CY1G4, Biolegend) for microscopy, anti-TfR (rb, 131135, Cell Signaling Technology) for western blotting, anti-EEA1 (ms, clone 14, BD Biosciences), and anti-Rab11 (rb, clone D4F5, CST).

### *2.10.2 Cell culture, transfection, and knockdown*

HeLa, T-REx<sup>TM</sup>- HeLa, and HeLa stable cell lines were maintained at 37°C, 5% CO<sub>2</sub> in DMEM (Corning) supplemented with 10 % FBS, 100 U/mL penicillin-streptomycin, and 2 mM L-glutamine. Cells were transfected at 80% confluency with 1 µg of each plasmid using Lipofectamine 2000 or Lipofectamine 3000 (Thermo Fisher Scientific) according to the manufacturer's instructions. Knockdown experiments were performed by reverse transfecting 5 x 10<sup>4</sup> cells in a 24-well plate with 6 pmol ATG9A SMARTpool siRNA (Dharmacon) and

Lipofectamine RNAiMAX. After 48 h, Vx3 expression was induced with 1  $\mu\text{g}/\text{mL}$  Dox.

Analyses were performed 24 h later.

The Flp-In T-Rex system (Thermo Fisher) was used for stable integration of 3xFLAG-Vx3NB-EGFP or 3xFLAG-Vx3-EGFP in T-REx-HeLa cells. This system allows for specific activation of transcription by blocking gene expression from CMV promoters through tetracycline operators and repressors. The parental cells were co-transfected with the appropriate Vx3 constructs in pcDNA5/FRT/TO and Flp recombinase vector pOG44. Single clones were selected under 0.3 mg/mL hygromycin to choose one that had high Vx3 expression and formed robust Vx3 foci when using 1  $\mu\text{g}/\text{mL}$  Dox for 24 or 48 h. To create 3xFLAG-Vx3-EGFP stable HeLa cells that also constitutively express VMP1-HA-iRFP, Phoenix cells were co-transfected with the retroviral plasmid pQCXIP VMP1 and VSV-G envelope expressing plasmid pCS1.G (a gift from Jennifer DeLuca, Colorado State University). The resulting retrovirus was used to infect HeLa 3xFLAG-Vx3-EGFP under 1  $\mu\text{g}/\text{mL}$  puromycin selection. Both stable cell lines were generated by Francesco Scavone. Stable HeLa 3xFLAG-Vx3-EGFP VMP1-HA-iRFP cells were then sorted for monoclonal by FACS (MoFlo) to screen for high EGFP and iRFP expressing cells.

Cell lines were checked for mycoplasma contamination by DAPI staining and using the PCR Mycoplasma Detection Kit (G238, Applied Biological Materials Inc.).

### *2.10.3 Co-immunoprecipitation*

Vx3 stable cells were induced with 1  $\mu\text{g}/\text{mL}$  Dox for 48h and lysed in RIPA lysis buffer (50 mM Tris-Cl pH 7.6, 300 mM NaCl, 1% NP-40, 0.1% sodium deoxycholate, 1 mM EDTA) with 100 mM iodoacetamide, 4 mM 1,10-phenanthroline, and a protease inhibitor cocktail (P8340, Sigma-Aldrich). For co-IP, 15  $\mu\text{L}$  GFP Trap agarose resin (ChromoTek) was added per

10 cm dish of cells. For binding, salt was increased to 500 mM NaCl, and samples were incubated at 4°C for 1-2 h on a tube revolver. The resin was then washed with TBS (50 mM Tris pH 7.6, 150 mM NaCl). Samples were first eluted in 1.5x resin volume of elution buffer (50 mM Tris pH 7.6, 3.3% SDS, 2 mM DTT) at room temperature followed by a second round of elution by heating at 70°C. The majority of the ubiquitinated proteins were in the first elution, and the second elution mostly contained Vx3.

#### *2.10.4 Mass spectrometry sample preparation*

For the first mass spectrometry experiment, 4 x 10 cm dishes per condition were prepared. After co-IP, the elutions were precipitated in 80% acetone at -80°C overnight. The protein pellets were recovered by centrifuging at 10,000 x g, 4°C for 30 min and resuspended in 2x Laemmli Sample Buffer. To further fractionate the samples, 90% of the elutions were run on a 4-15% SDS-PAGE gel (456-1083, Bio-Rad) past the stacking gel. The gel was then stained (0.05% Coomassie Blue R250, 10% acetic acid, 50% MeOH) for 1 h and destained (10% acetic acid, 50% MeOH) for 3 h with a solvent change each hour to remove SDS. Each sample was extracted and separated into two pieces to separate proteins <70 kDa and >70 kDa. The gel was dehydrated, reduced, and alkylated: 100% acetonitrile for 5 min at room temperature, 10 mM DTT with 0.1 M ammonium bicarbonate for 20 min at 55°C, 100% acetonitrile for 5 min, 55 mM iodoacetamide for 20 min at room temperature, and 100% acetonitrile for 5 min. The samples were then rehydrated and digested with 1:30 trypsin (V5111, Promega) in 0.1 M ammonium bicarbonate with 0.01% ProteaseMAX (V2071, Promega) at 37°C overnight. Afterwards, the reactions were stopped with 10% TFA, and the supernatant was collected. Remaining peptides left in the gel were further extracted by shaking the gel pieces in 50%

acetonitrile and 0.1% TFA for 2 h and 100% acetonitrile for 5 min. These solutions were combined and dried down in a vacuum centrifuge.

For the second mass spectrometry experiment, 3 x 15 cm dishes per condition were prepared. To induce for autophagy, 45 uL of Lipofectamine 3000 was added per 15 cm dish. After co-IP, the elutions were acetone precipitated at -20°C overnight. The proteins were recovered after washing with 80% acetone and then 100% acetone, centrifuging at 11700 x g, 4°C for 15 min. The pellets were resuspended in 50 mM Tris-Cl pH 7.6, 150 mM NaCl, 8 M urea. Only the samples from the first elution were analyzed. To neutralize, reduce, and alkylate the samples: ammonium bicarbonate was added to a final concentration of 12.3 mM, TCEP was added to a final concentration of 2.8 mM at 55°C for 15 min, and iodoacetamide was added at 2.7 mM for 30 min at room temperature. The samples were diluted to contain 2 M urea before adding 1:30 trypsin and incubating at 37°C overnight. The proteins were then further diluted to have 1 M urea. Another aliquot of trypsin was added at 37°C for 3 h. The peptides were then acidified in a final concentration of 20 mM NH<sub>4</sub>COOH and separated on a Phenomenex Gemini® 3 µm C18 110 Å LC 30 x 2 mm (00A-4439-B0) reverse phase column. The elution was set to an 80% gradient of elution buffer (20 mM NH<sub>4</sub>COOH, 50% acetonitrile) spanning 80 min. The fractionated elutions were dried down in a vacuum centrifuge.

After the peptides were prepared, they were sent to the University of California, San Francisco Mass Spectrometry Facility for LC-MS/MS analysis.

#### *2.10.5 Biochemical assays*

For DUB assays, immunoprecipitated samples were directly digested while still bound to GFP Trap agarose resin. After washing the resin but before elution, the resin was resuspended in digestion buffer (PBS pH 7.4, 0.3 mg/mL ovalbumin, 0.05% Brij35, 5 mM DTT). Digestions

were incubated with 10  $\mu$ M of different DUBs at 37°C for at least 1.5 h with shaking: OTUB1 (a gift from Cynthia Wolberger, Johns Hopkins University), GST-AMSH (a gift from Tingting Yao), and USP2cc<sup>26</sup> (a gift from Bob Cohen). The samples were then eluted with 2x Laemmli Sample Buffer. Glycosidase treatments followed USP2cc digestions of samples before elution. Endo HF (P07035, NEB) and PNGase F (P0708S, NEB) were used according to manufacturer's instructions.

#### *2.10.6 Gel electrophoresis and immunoblotting*

Samples were never boiled for SDS-PAGE to avoid aggregation of membrane proteins. This practice was initially used for ATG9A<sup>27</sup> but was carried forward after LC-MS/MS revealed that the ubiquitinated proteins were transmembrane proteins. For western blots, primary antibodies were used at a 1:1000 dilution in 1% milk. The polyvinylidene difluoride membranes were then immunoblotted with fluorescent secondary antibodies and imaged with a LI-COR Biosciences Odyssey CLx scanner.

#### *2.10.7 Internalization assays*

After 24 h Vx3 expression induced by 1  $\mu$ g/mL Dox, the growth media was supplemented with 50  $\mu$ g/mL CF@640R-conjugated human transferrin (00085, Biotium) for 2 h or 1:100 anti-MHC-I antibody for 1 h before fixation.

#### *2.10.8 Immunostaining and microscopy*

For microscopy, cells on coverslips were fixed with 2.5% paraformaldehyde in PBS for 10 min at 37°C. The cells were then permeabilized with 0.1% Triton X-100 for 10 min at room temperature and blocked for 30 min with 1% BSA in PBS. All primary antibodies were diluted 1:200 in 1% BSA and incubated with cells for 2 h at room temperature or overnight at 4 °C, Coverslips were incubated with secondary antibodies for 1 h at room temperature. Imaging was

performed on a LSM 880 confocal microscope (Zeiss) using the Plan-Apo 63x/1.4 Oil DIC objective. Images were captured using line scanning and processed using ZEN 2.3.

## CHAPTER 3: DISABLING Vx3

### 3.1 Introduction

While Vx3 is a useful tool for identifying and trapping K63-polyUb, its utility can be furthered by incorporating the ability to induce K63-polyUb release. Inducibly disabled Vx3 lends the opportunity to study immediate downstream activities mediated by K63-polyUb. To incorporate controlled release of K63-polyUb, Vx3 was modified through different approaches. Modifying Vx3 using an existing inducible dimerization system succeeded in causing Vx3 to release bound K63-polyUb in vitro, essentially disabling the sensor. Alternatively, Vx3 was integrated into a reversible ligand-controlled degradation system, and two different protocols were developed for tuning the sensor's expression and degradation.

### 3.2 Chemically-induced dimerization

Chemically-induced dimerization (CID) systems consist of a pair of proteins that don't normally interact but rapidly dimerize with high affinity in the presence of a specific ligand. These CID proteins can be fused to proteins of interest to manipulate their association or localization in the cell. Utilizing CID to induce specific cellular localization is useful for purposes such as affinity modulation, activation of cascade pathways, and transcriptional control.<sup>28</sup> The rapamycin-mediated CID system consists of the 12 kDa FK506-binding protein 12 (FKBP12) and the 11 kDa human FKBP-rapamycin binding domain (FRB).<sup>29</sup> The mammalian target of rapamycin (mTOR) is a central metabolic regulator, and FRB is derived from its rapamycin binding domain. mTOR is an incredibly large protein at 289 kDa, so difficulties can arise when cloning genetic fusions. Also, its large size may interfere with induced binding events, so only mTOR's rapamycin binding domain is retained for the CID system. At 11 kDa,

FRB is much easier to manage.<sup>28,29</sup> The dimerizing ligand rapamycin is an immunosuppressive compound. All components bind to each other with incredibly high affinity, with  $K_d$  ranging from low  $\mu\text{M}$  to  $\text{fM}$ .<sup>30</sup> FKBP12-rapamycin-FRB is an attractive CID system due to the small protein sizes and its strong affinity.

### **3.3 Adapting FKBP12-rapamycin-FRB for Vx3**

Vx3 was fused to the N-terminus of FRB, the smaller protein of the dimerizing pair, to minimize hindrances to the sensor's ability to bind K63-polyUb (FIG 3.1). The crystal structure of the FKBP12-rapamycin-FRB complex indicates that rapamycin binds between the two proteins at an interface formed by their C-termini while both N-termini face outward to the cytosol in cells.<sup>31,32</sup> Fusing Vx3 at FRB's N-terminus rather than the C-terminus avoids potentially interfering with FRB's dimerization with FKBP12 due to Vx3's possible steric clash with rapamycin.

While fusing Vx3 to FRB causes it to localize with FKBP12 upon rapamycin addition, this activity alone does not result in K63-polyUb release. In order to contribute a disrupting interaction, UbK0 was fused to the N-terminus of FKBP12. UbK0 is an Ub molecule with all lysines mutated to arginine residues to prevent further ubiquitination that would complicate this system; additionally, a G76V mutation serves to avoid cleavage by deubiquitinating enzymes. The purpose of this protein is to compete with K63-polyUb chains in binding to the sensor. Upon rapamycin addition, FRB and FKBP12 will dimerize and bring UbK0 and Vx3 binding K63-polyUb in close proximity, allowing UbK0 to interact with one of the UIMs in Vx3. With only two UIMs available to bind K63-polyUb, the affinity between Vx3 and K63-polyUb will be reduced  $\sim 300$ -fold.<sup>33</sup> As UbK0 binds to Vx3, the sensor's high affinity for K63-polyUb is

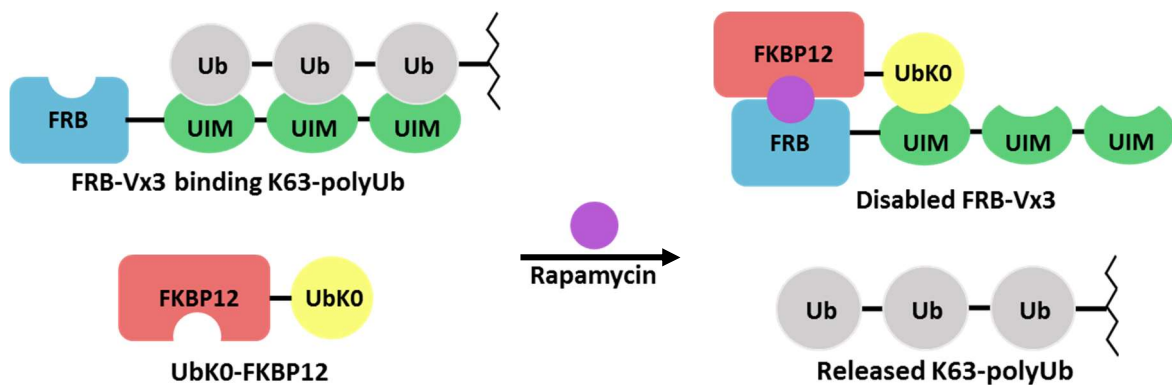


**FIG 3.1 Schematic of the FKBP12-rapamycin-FRB CID system adapted for Vx3.** The system consists of fusion proteins FRB-Vx3 and UbK0-FKBP12. In the absence of dimerizing ligand rapamycin, FRB-Vx3 can bind K63-polyUb that is modifying another protein. Upon rapamycin addition, FRB and FKBP12 dimerize, allowing UbK0 to come into close proximity with one of Vx3's UIMs. The competition for binding to Vx3 causes Vx3 to release the K63-polyubiquitinated protein and remain unable to bind K63-polyUb again while rapamycin remains in the system.

compromised, effectively disabling the sensor and allowing bound K63-polyUb chains to be released.

To ensure that modifying Vx3 doesn't compromise its high affinity for K63-polyUb, FRB-Vx3 and UbK0-FKBP12 were expressed in *E. coli* and purified for in vitro binding assays. Fluorescence polarization assays were chosen to measure binding affinities. In a fluorescence polarization assay, a fluorescently-labeled protein emits a certain amount of radiation when exposed to polarized light. The radiation changes when the fluorescently-labeled protein changes in size and shape upon binding another protein that's unlabeled.<sup>34</sup> A competition assay was set up containing K63-triUb and fluorescein-labeled Vx3; formation of this complex is competed by increasing amounts of unlabeled FRB-Vx3 (FIG 3.2.A). FRB-Vx3's high affinity for K63-triUb was slightly lower but still acceptable at  $K_i = 25.2$  nM (FIG 3.2.B) compared to Vx3 ( $K_d = 7.4$  nM).<sup>5</sup> As FKBP12-rapamycin-FRB has incredibly high affinity with femtomolar  $K_d$ , it was difficult to assess whether there were any changes in the affinity between FRB-Vx3 and UbK0-FKBP12 in the presence of rapamycin compared to the original CID system.

There were unexpected solubility issues observed in UbK0-FKBP12 purified from bacteria. When the purified protein was on ice, the solution would become cloudy. But, when warmed to room temperature, Ubk0-FKBP12 was soluble again. This problem was eliminated when the 2 mM UbK0-FKBP12 solution was diluted to 0.6 mM. UbK0 is very soluble alone, so FKBP12 solubility may be limited when expressed in HeLa cells.

### **3.4 FRB-Vx3 is partially disabled in vitro by UbK0-FKBP12 and rapamycin**

By modifying Vx3, the goal was to inhibit its binding to K63-polyUb when UbK0-FKBP12 and rapamycin are added. A competition binding assay was used to test whether FRB-

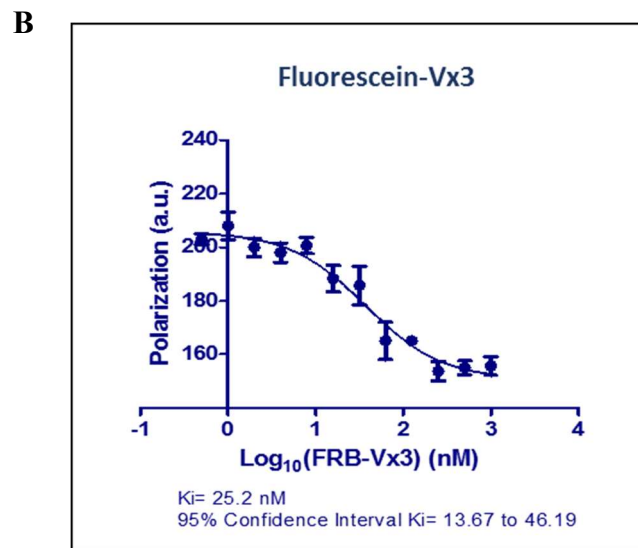
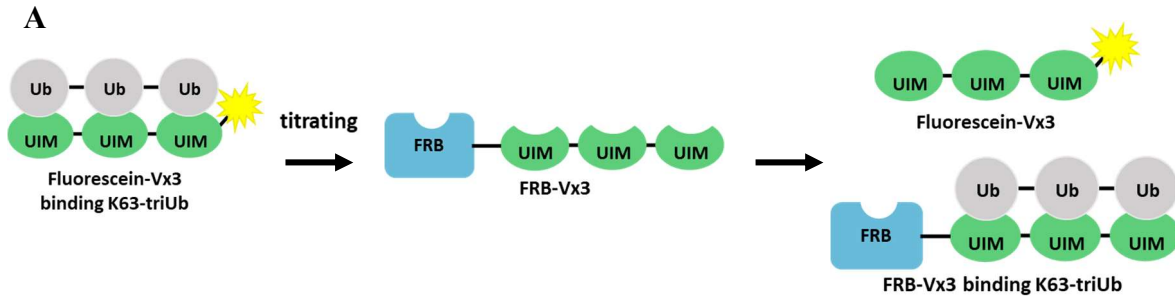


**FIG 3.2. FRB-Vx3 has high affinity for K63-polyUb.** (A) The schematic depicts the assay set-up for a fluorescence polarization assay to determine FRB-Vx3's affinity for K63-triUb. Fluorescently labeled Vx3 bound K63-triUb, but as FRB-Vx3 was titrated and competed with fluorescein-Vx3 for binding to K63-triUb, unbound fluorescein-Vx3 had decreased polarization. (B) Fluorescence polarization measurements were performed with 7 nM fluorescein-Vx3, 10 nM K63-triUb, and increasing concentrations of FRB-Vx3. The experiment was performed with three replicates.

Vx3 can be successfully disabled. The assay measured fluorescence polarization of fluorescein-Vx3 in the presence of K63-triUb, an excess of FRB-Vx3, rapamycin, and an increasing molar ratio of UbK0-FKBP12 compared to FRB-Vx3 (FIG 3.3.A). At a 10:1 molar ratio of UbK0-FKBP12 to FRB-Vx3, only 65% of the entire population of FRB-Vx3 released K63-triUb (FIG 3.3.B). There was not an appreciable improvement in K63-triUb release correlating with increasing concentrations of UbK0-FKBP12 in the presence of rapamycin. Thus, Ubk0-FKBP12 wasn't able to completely disable FRB-Vx3.

### **3.5 2UbK0-FKBP12 and rapamycin disables FRB-Vx3 in vitro**

To enhance binding to the Vx3 moiety of FRB-Vx3, a second UbK0 was added to UbK0-FKBP12 with the hope that this would confer greater ability to compete with K63-polyUb in binding to Vx3 (FIG 3.1.B). The two Ub mutants were connected with a two-amino acid, flexible Ser-Gly linker. During purification, 2UbK0-FKBP12 was even less soluble than UbK0-FKBP12; the protein exhibited the same cloudy features on ice but was clear when the 400  $\mu$ M 2UbK0-FKBP12 stock was diluted to 120  $\mu$ M. To test whether 2UbK0 is contributing to the solubility issue, 2UbK0 alone was overexpressed in bacteria; it was insoluble (data not shown), so fusing 2Ubk0 to FKBP12 may further limit the protein's solubility.

In the same fluorescence polarization experiments as those with UbK0-FKBP12, 2UbK0-FKBP12 showed greater ability to inhibit FRB-Vx3 from binding K63-triUb (FIG 3.3.A, B). A 1:1 molar ratio wasn't enough to completely prevent FRB-Vx3 binding, but at two times more 2UbK0-FKBP12 than FRB-Vx3, the sensor was already 88% inhibited. Increasing the molar ratio of FRB-Vx3 to FKBP12 to 1:5 caused 97% of all FRB-Vx3 to release K63-triUb. In this experiment, measurements were taken at 1 h incubation at room temperature. Shorter incubation times were also tested using the same protein concentrations. Only 53% of FRB-Vx3 was

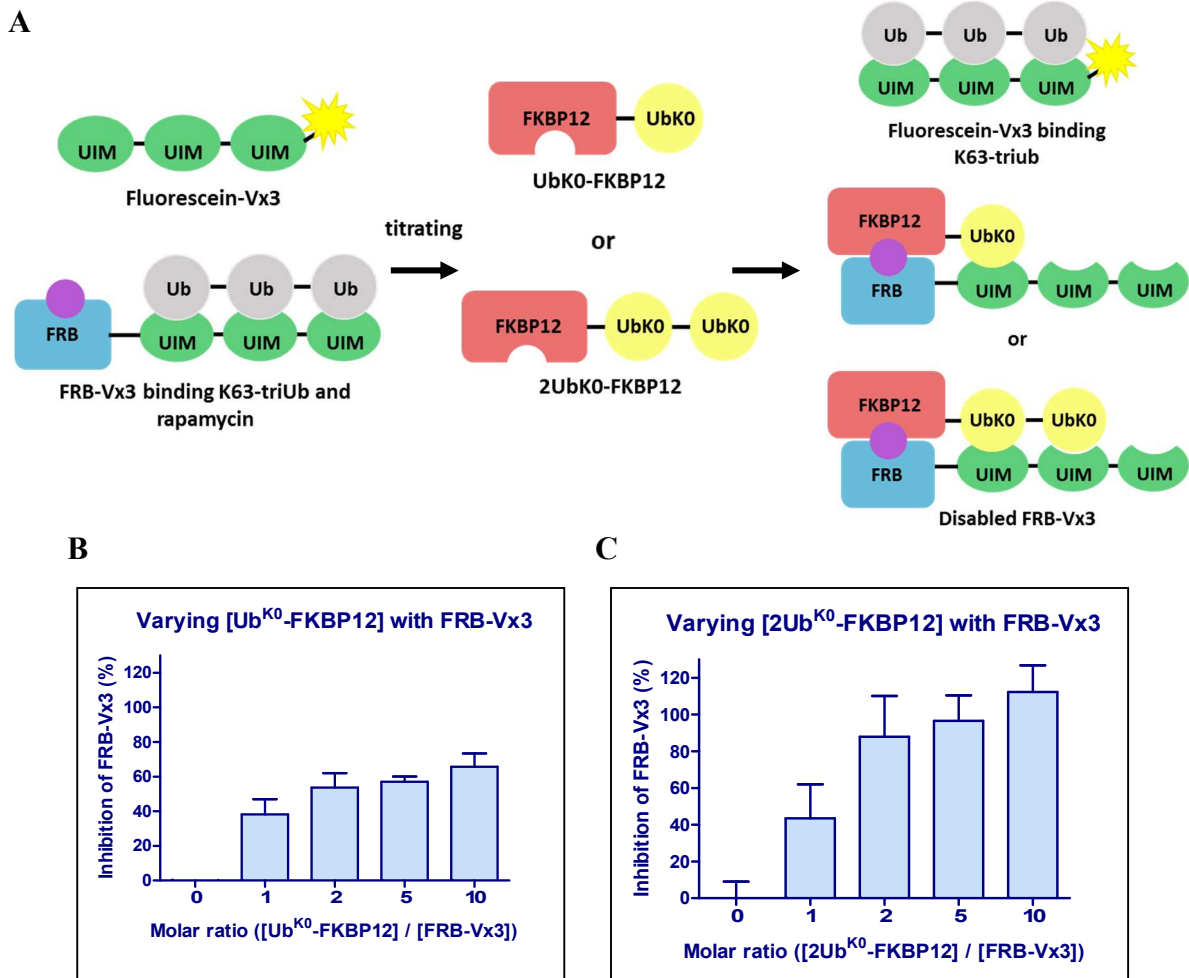


**FIG 3.3. 2UbK0-FKBP12 and rapamycin can disable FRB-Vx3.** (A) The graphic depicts a competition binding assay using fluorescence polarization to determine how well the rapamycin system works to induce FRB-Vx3 to release K63-triUb. The assay was performed with excess FRB-Vx3 compared to fluorescein-Vx3 so that most of the K63-triUb is bound by FRB-Vx3. Rapamycin was already present to mediate FRB and FKBP12 dimerization. Upon titrating UbK0-FKBP12 or 2UbK0-FKBP12, it dimerized with FRB-Vx3, and the competing interaction presumably caused FRB-Vx3 to release K63-triUb. When fluorescein-Vx3 bound free K63-triUb, the new protein interaction increased its fluorescence polarization. Higher fluorescein-Vx3 polarization equated to more disabled FRB-Vx3. (B) The binding assay consisted of 7 nM fluorescein-Vx3, 10 nM K63-triUb, 63.1 nM FRB-Vx3, 1  $\mu$ M rapamycin, and increasing concentrations of UbK0-FKBP12 or 2UbK0-FKBP12. The polarization values were normalized and transformed using a scaling equation described in the methods. This equation set 100% of FRB-Vx3 being disabled as the polarization value when all fluorescein-Vx3 were binding K63-triUb. These experiments were completed in triplicate.

disabled after 20 min incubation, and 86% of FRB-Vx3 was disabled after 40 min incubation (data not shown). Although 2UbK0-FKBP12 has some solubility problems when expressed in bacteria, it is better than Ubk0-FKB12 at disabling FRB-Vx3. If 2UbK0-FKBP12's solubility problems can be attributed to difficulties in folding, it is possible that expression in mammalian cells, which have more sophisticated chaperones than bacteria, will help alleviate the issue.

### **3.6 FRB-Vx3 binds endogenous K63-polyUb in mammalian cells**

FRB-Vx3-EGFP expression in HeLa cells exhibited foci formation characteristic of Vx3 (FIG 3.4.A), presumably because FRB-Vx3 was able to bind endogenous K63-polyUb chains. One concern about this CID system is that rapamycin inhibits mTOR which is a popular target for inducing autophagy.<sup>35</sup> However, adding 1  $\mu$ M rapamycin did not affect foci formation.

### **3.7 2UbK0-FKBP12 forms K63-polyUb-positive aggregates**

In order to express more 2UbK0-FKBP12 than FRB-Vx3 at a 2:1 molar ratio, the constructs were subcloned into mammalian vectors with attenuated CMV promoters. pCMV WT expresses double the amount of protein expressed by pCMV  $\Delta$ 3.<sup>36</sup> When co-transfecting plasmids to express pCMV WT 2UbK0-FKBP12-iRFP and pCMV  $\Delta$ 3 FRB-Vx3-EGFP in HeLa cells, 2UbK0-FKBP12-iRFP already formed foci prior to rapamycin addition (data not shown). The expectation was to see 2UbK0-FKBP12-iRFP diffused throughout the cell because it is specific to FRB-Vx3 and shouldn't be bound to anything yet. When expressing pCMV WT 2UbK0-FKBP12-iRFP alone, foci still formed, and they co-localized with K63-polyUb (FIG 3.4.B). Given that 2UbK0 had solubility problems, FKBP12-iRFP was expressed alone in HeLa cells to determine if 2UbK0 was the culprit. However, FKBP12-iRFP also exhibited the same phenotype, so the problem may stem from FKBP12 or the iRFP tag. When cells cannot clear

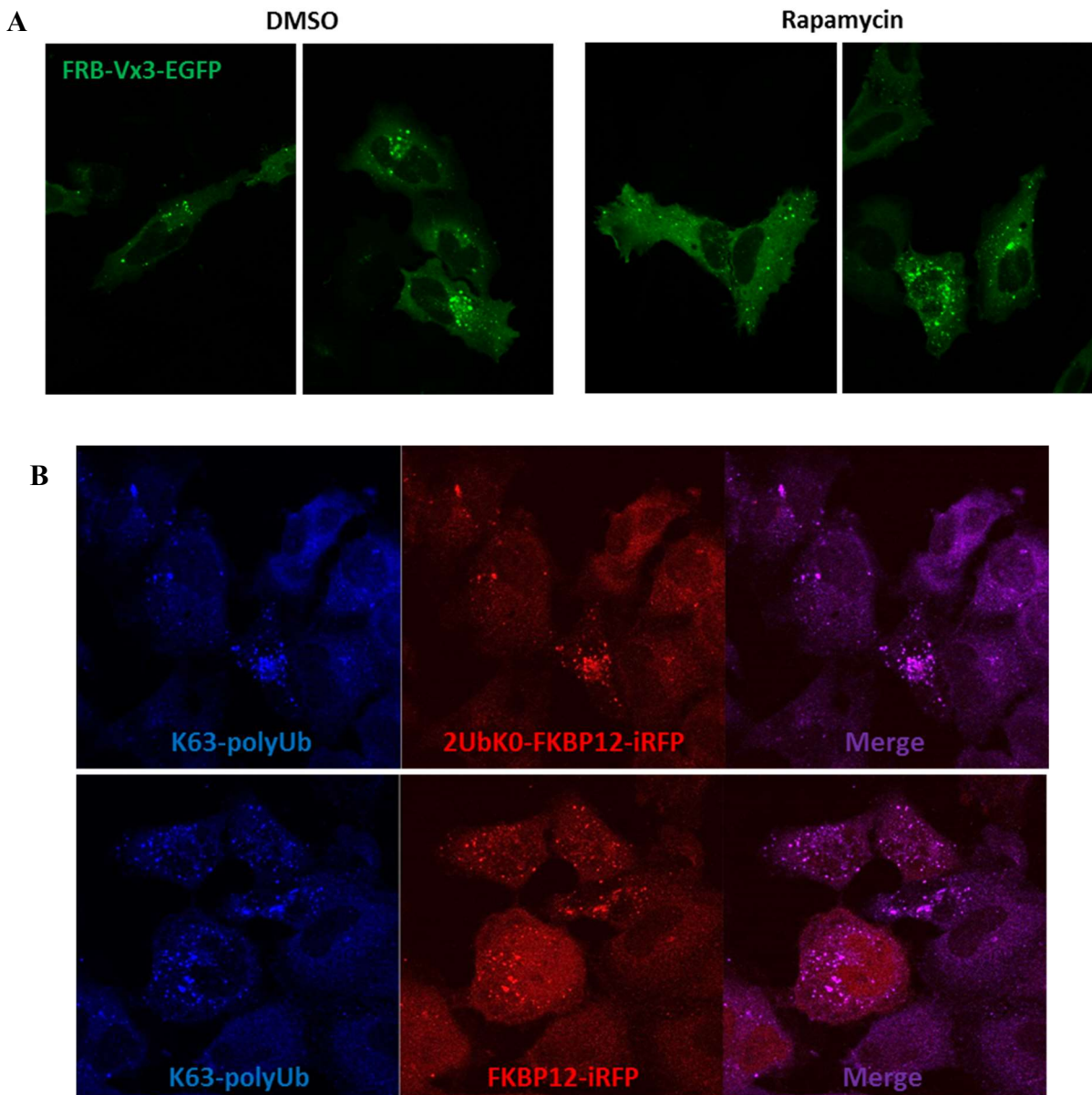


**FIG 3.4 FRB-Vx3 binds endogenous K63-polyUb, but FKBP12 localizes into K63-polyUb-positive foci.** (A) FRB-Vx3 transfected in HeLa cells formed foci similar to those from Vx3. Adding 1  $\mu$ M rapamycin for 1 h didn't affect foci formation. Francesco Scavone assisted with microscopy. (B) In HeLa cells, transfected 2UbK0-FKBP12-iRFP, in the absence of FRB-Vx3 and rapamycin, formed foci that co-localized with endogenous K63-polyUb. Transfecting FKBP12-iRFP without the 2UbK0 fusion also resulted in the same phenotype.

misfolded proteins efficiently, the proteins form cytoplasmic aggregates which are sequestered into aggresomes; it is known that unanchored K63-polyUb chains are involved.<sup>37</sup> Issues with correct FKBP12-iRFP folding may be the culprit for foci that co-localize with K63-polyUb. The rapamycin CID system works well in vitro but still needs work for use in cells.

### **3.8 Alternative CID systems**

After the rapamycin CID system proved unsuccessful, other systems were tested including gibberellin-GID1-GAI<sup>38</sup> and DHFR-bis-MTX-DHFR.<sup>39</sup> None of the constructs were promising and couldn't be moved past in vitro testing because they did not successfully disable Vx3. None of the other CID systems possess the incredibly high affinity and rapid binding offered by the rapamycin system.

### **3.9 A degradation system to modulate protein levels**

Protein degradation systems typically take advantage of cellular degradative machinery to turnover targeted proteins. These systems offer reproducible and tunable control over cellular levels of proteins of interest. The destabilizing domain (DD), a mutant of FKBP12, is unstable following translation and is targeted for proteasomal degradation. Expressing DD as a fusion tag on any protein can target the protein for degradation. Upon addition and binding of stabilizing ligand Shield1, DD is stabilized and shielded from degradation.<sup>40,41</sup>

### **3.10 Adapting DD for Vx3**

In order to adapt DD for Vx3 degradation, DD was fused to the N-terminus of 3xFLAG-Vx3-EGFP and cloned into the pcDNA5/FRT/TO plasmid, which allows Dox-inducible protein expression. Typically, transfecting plasmids with high expression promoters result in overexpression of the encoded proteins, which could overwhelm the ubiquitination and degradation machinery. This system required careful fine tuning because there needed to be a

balance between allowing sufficient DD-Vx3 to stabilize after Dox and Shield1 addition in order to form foci while not accumulating so much to ensure efficient degradation of DD-Vx3. For rapid build-up of DD-Vx3, 1  $\mu\text{g}/\text{mL}$  Dox and 100  $\mu\text{M}$  Shield1 were added 23 h after transfection before wash out 1 h later. For slow build-up of DD-Vx3, 1  $\text{ng}/\text{mL}$  Dox was added when transfecting cells, and 100  $\mu\text{M}$  Shield1 was added 12 h later. For both methods, Shield1 was washed out at 24 h post transfection to initiate DD-Vx3 degradation. Both methods worked well, although the rapidly stabilized DD-Vx3 was degraded much quicker with most of the sensor eliminated 2 h after wash out compared 12 h for the slow build-up method (data not shown).

### **3.11 Labeling of HaloTagged proteins at DD-Vx3 foci**

Using this degradation system, the intent was to co-transfect DD-Vx3-EGFP with a fluorescently labeled protein of interest such as TfR. When Vx3 was stabilized, it was easy to see the subset of TfR that was ubiquitinated and trapped in Vx3 foci. However, upon Vx3 degradation, it was difficult to differentiate which TfR foci were originally co-localized with Vx3 apart from the majority of TfR which localizes to the plasma membrane or in small, cytosolic non-Vx3 foci. To get around this problem, HaloTag was fused to TfR. Proteins with a HaloTag are visualized with the addition of fluorescent HaloTag ligands.<sup>42</sup> In order to differentiate Vx3-associated TfR, a photoactivatable pA-JF-646-HaloTag ligand<sup>43</sup> was added to the cells. TfR-HaloTag specifically co-localizing with Vx3 foci can be visualized alone by activating pA-JF-646-HaloTag at Vx3 foci (FIG 3.5.A). To demonstrate the specificity of the visualized TfR by this method, cells were also dually labeled with an already activated ligand JF-549-HaloTag which shows the entire TfR population.

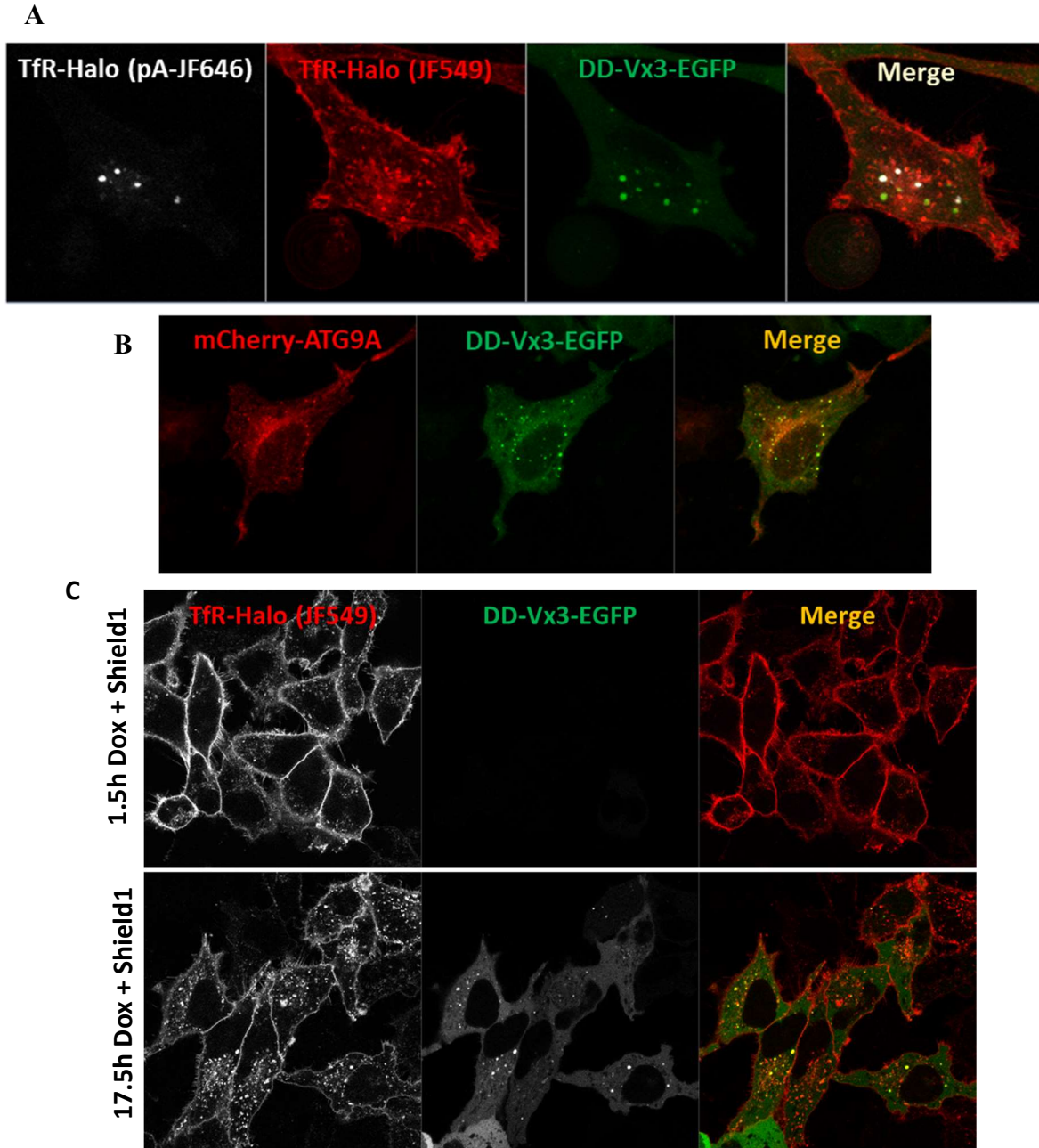


**FIG 3.5. ATG9A and TfR accumulate at DD-Vx3 foci on different time-scales.** T-REx™-HeLa cells were transfected with DD-3xFLAG-Vx3-EGFP. (A) The cells were co-transfected with TfR-HaloTag following the slow build-up protocol. TfR was dually labeled with HaloTag ligands JF-549 and pA-JF-646. A subset of TfR co-localizing with DD-Vx3 was photoactivated. This experiment was performed by Francesco Scavone. (B) After co-transfection with mCherry-ATG9A following the rapid build-up protocol, images were taken at 1 h post DD-Vx3 stabilization. (C). TfR-HaloTag was co-transfected following the rapid protocol. Due to low DD-Vx3 levels, normalization makes it appear as though there are no DD-Vx3 foci at 1.5 h post stabilization.

### 3.12 Dynamics at Vx3 foci

It was interesting to find that the dynamics of ATG9A were very different from TfR at Vx3 foci. To image ATG9A after DD-Vx3 degradation, the rapid DD-Vx3 build-up protocol was followed because HaloTag-ATG9A co-localized well with DD-Vx3 foci after 1 h of Dox and Shield1 addition when foci are barely detectable (FIG 3.5.B). However, the rapid DD-Vx3 build-up protocol didn't work well for imaging TfR because it took 12-16 h after DD-Vx3 stabilization for TfR to accumulate at Vx3 foci at detectable levels (FIG 3.5.C). The quick build-up protocol wasn't compatible for imaging TfR after DD-Vx3 degradation because 16 h of 1  $\mu\text{g}/\text{mL}$  Dox with Shield1 accumulated too much DD-Vx3 to be degraded efficiently. The slow DD-Vx3 build-up protocol with a lower concentration of Dox was developed in order to visualize downstream ubiquitinated protein activity after DD-Vx3 degradation. TfR required a surprisingly long time to accumulate at Vx3 foci.

### 3.13 Discussion

This chapter detailed the development of two methods for disabling or degrading Vx3 with fine control afforded by specific ligands. While the rapamycin system requires further work, in principle, it would be preferable over the degradation system. The main reason is that CID systems are rapid, whereas degradation systems typically require a long period for ubiquitination and proteolysis to occur. Degradation systems are rate-limited by the amount of cellular machinery available. The rapamycin system was able to disable FRB-Vx3 using 2UbK0-FKBP12 within 40 min *in vitro*, and tuning sensor expression levels is much simpler using attenuated CMV promoter plasmids to vary the amount of mRNA transcribed. The problem lies in FKBP12-iRFP forming foci and co-localizing with endogenous K63-polyUb in cells, indicating protein misfolding which may have led to aggregation. The aggregation may also be

caused by iRFP, specifically iRFP682, which forms a stable dimer.<sup>44</sup> However, it's possible that the system may work even if a subset of 2UbK0-FKBP12 is aggregated. An additional experiment with co-transfection of 2UbK0-FKBP12-iRFP and FRB-Vx3-EGFP would show whether adding rapamycin could still disperse Vx3 foci. If this system works, imaging ubiquitinated proteins would likely still require the dual HaloTag labeling described for DD-Vx3 to differentiate the subset of foci originally co-localizing with FRB-Vx3. The DD-Vx3 system is successful, although a bit difficult to implement and slow to release K63-polyUb.

### **3.14 Materials and methods**

#### *3.14.1 Plasmids*

The constructs FRB-Vx3, Ubk0-FKBP12, and 2UbK0-FKBP12 were designed by Yun-Seok Choi. They were cloned into pET28p vectors with 6xHis-tags for expression and purification in *E. coli* using FRB-N-TEV (Addgene #100095) and FKBP-C-TEV 219 (Addgene #100096), both gifts from Jim Wells (University of California, San Francisco), as templates. Plasmids were constructed by In-Fusion cloning (In-Fusion HD Cloning Kit, Clontech). Full construct sequences can be found in Appendix 2. For expression in mammalian cell culture, FRB-Vx3 was first subcloned into pEGFP-N1 through digestion with EcoRI and BamHI and ligation with TaKaRa DNA Ligation Kit Ver 2.1 (Clontech), and then FRB-Vx3-EGFP was subcloned into pCMVwt (wISP12-91) through In-Fusion cloning. 2UbK0-FKBP12-iRFP was also cloned into pCMV delta 3 (wISP12-94) through In-Fusion cloning. Both pCMVwt (wISP12-91) and pCMV delta 3 (wISP12-94) were gifts from Wes Sundquist (University of Utah).<sup>36</sup> For DD, FKBP12 E31G, F36V, R71G, K105E<sup>41</sup> was ordered as a gBlock (IDT) for In-Fusion cloning into pcDNA5/FRT/TO 3xFLAG-Vx3-EGFP at the N-terminus of 3xFLAG. ATG9A was cloned from cDNA by Francesco Scavone into pFN21A-HaloTag. TfR-HaloTag

was constructed by replacing mCherry in the plasmid mCherry-TFR-20 (Addgene #55144), a gift from Michael Davidson (Florida State University), with HaloTag using restriction sites BamHI and NotI.

### *3.14.2 Protein expression and purification*

All rapamycin system pET28p plasmids were transformed into *E. coli* BL21-CodonPlus(DE3) cells and expressed in 2xYT media with 0.1 mM IPTG at 16°C for 22 h. Harvested cells were resuspended in lysis buffer (20 mM NaPi, pH 7.4, 500 mM NaCl, 10 mM imidazole, and 10 mM 2-mercaptoethanol) supplemented with a protease inhibitor cocktail (P8340, Sigma-Aldrich), 20 µM DNase, 1 mM PMSF, and 0.5 mg/mL lysozyme. Cells were lysed by sonication with cooling on ice. After centrifuging at 20,200 x g for 30 min, the collected supernatant was applied to nickel resin (HisTrap HP, GE Healthcare), and proteins were eluted with lysis buffer adjusted to contain 350 mM imidazole. If needed, anion exchange chromatography (HiTrap Q HP, Amersham) was further used to purify the proteins with binding buffer (25 mM NaPi pH 8, 1 mM DTT) and elution buffer (25 mM NaPi pH 8, 1 M NaCl, 1 mM DTT). All purified proteins were finally exchanged to the same storage buffer (PBS, 1 mM DTT) and flash frozen with liquid nitrogen. K63-triUb was prepared as previously described.<sup>45</sup> Fluorescein-Vx3 was a gift from Yun-Seok Choi.

### *3.14.3 Fluorescence polarization binding assays*

Samples were prepared in binding assay buffer (PBS, 0.3 mg/ml ovalbumin, 0.05% Brij35, and 2 mM DTT), and fluorescence polarization was measured on a plate reader (Synergy 4, BioTek) after 1 h incubation at 25 °C. In the experiment to assess FRB-Vx3 inhibition with 1 µM rapamycin with increasing concentrations of UbK0-FKBP12 or 2UbK0-FKBP12, the

polarization values from fluorescein-Vx3 were normalized by a modified feature scaling equation to convert the scale of the polarization from [0, 1] to percentage of FRB-Vx3 inhibited:

$$100 - \frac{(F \sim Vx3 + Ub_3)^{pol} - (sample)^{pol}}{(F \sim Vx3 + Ub_3)^{pol} - (F \sim Vx3 + Ub_3 + FRB \sim Vx3)^{pol}} \times 100$$

The equation accounts for the polarization (pol) when all fluorescein-Vx3 ( $F \sim Vx3$ ) molecules are binding K63-triUb ( $Ub_3$ ) and the polarization before UbK0-FKBP12 or 2UbK0-FKBP12 is added.  $K_i$  was calculated using GraphPad Prism 6.

#### 3.14.4 Cell culture

HeLa and T-REx™- HeLa cells were cultured in DMEM supplemented with 10 % FBS and 100 U/mL penicillin-streptomycin, and 2 mM L-glutamine; 1 µg of each plasmid was transfected into 80% confluent cells using Lipofectamine 2000 or Lipofectamine 3000 (Thermo Fisher Scientific) according to manufacturer's protocol. Treatments with DMSO alone (control) or 1 µM rapamycin (from 1 mM stock in DMSO) were added 22 hours after transfection and fixed with 2.5% paraformaldehyde 24 hours after transfection on glass coverslips.

For a slow build-up of DD-Vx3, 1 ng/mL Dox added simultaneously when transfecting T-REx™- HeLa cells; after 12 h, 100 µM Shield1 was added. After 24 h post transfection, Shield1 and DD-Vx3 can be washed out to initiate degradation. For a rapid build-up of DD-Vx3, 1 µg/mL Dox and 100 µM Shield1 were added 1 h before wash out. Cells were washed thrice with PBS.

#### 3.14.5 Fluorescence microscopy

For FIG 3.4.A, microscopy was performed using an Olympus IX81 spinning disk confocal (CSU22 head) microscope with 100x/1.40 NA objective, using a 488 nm laser to excite EGFP and a 561 nm laser to excite iRFP. Fluorescent images were acquired with a Photometrics Cascade II CCD camera using SlideBook (Intelligent Imaging Innovations) software.

Microscopy for FIG 3.4.B was performed for fixed cells immunostained using anti-K63-polyUb antibody (Apu3, Millipore) following the immunostaining and microscopy protocol detailed in Chapter 2.

For DD-Vx3, live cells were imaged in live-cell imaging media (FluoroBrite DMEM; A1896701, Thermo Fisher) supplemented with 10 % FBS and 100 U/mL penicillin-streptomycin, and 2 mM L-glutamine. HaloTagged constructs were labeled with 90 nM of pA-JF646-HaloTag and 10 nM JF-549-HaloTag ligands, both gifts from Luke Davis (Howard Hughes Medical Institute). Labeling occurred at 37°C, 5% CO<sub>2</sub> for 30 min, and cells were then washed out 3x with PBS for the quick DD-Vx3 protocol or left in live-cell imaging media for the long protocol. Imaging was performed on a LSM 880 confocal microscope (Zeiss) using the Plan-Apo 63x/1.4 Oil DIC objective and incubated at 37°C, 5% CO<sub>2</sub> for live-cell imaging. Images were captured using line scanning and processed using ZEN 2.3.

## CHAPTER 4: CONCLUSIONS

This thesis sought to provide additional insights into the nature and fate of K63-polyubiquitinated proteins that accumulate in Vx3 foci through a mixture of biochemical and microscopy-based experiments. While many mysteries still remain regarding Vx3 foci, this study revealed that Vx3 binds K63-polyubiquitinated transmembrane proteins (e.g. TfR) which were unconventionally trafficked from the ER and likely involved in a new quality control pathway that is stalled near lysosomes due to Vx3 inhibiting K63-polyUb signaling.

Results from the mass spectrometry experiments now offer a plethora of proteins to follow up with. This is especially true for the second experiment which identified close to 5000 proteins. A very brief list focused on proteins with the most abundant peptides (TABLE 2.2). The complexity of this dataset possibly results from Vx3 binding all K63-polyUb chains in the cell. Vx3 foci only account for a small fraction of K63-polyUb populations, while diffused Vx3 may also bind K63-polyUb. All proteins of interest have to be individually screened to determine if they co-localize with Vx3 foci, whether they are K63-polyubiquitinated, and/or if they mediate Vx3 foci formation. Based on the biochemical and microscopy results, Vx3 foci may represent an intermediate stage of a transmembrane protein quality control pathway. Many proteins identified in the LC-MS/MS results can either be cargos, if ubiquitinated, or players of this poorly understood pathway, which is distinct from ERAD and intertwined with autophagy.

In the future, different sample preparation methods for mass spectrometry can be used to identify proteins directly interacting with Vx3. There are several proximity-based labeling methods that can be adapted to Vx3 where any proteins in close proximity can be labeled and identified by mass spectrometry. This approach may yield results that can complement and offer

clarity on the previous LC-MS/MS results based on Vx3 co-IP, but it still does not exclude Vx3-associated proteins outside of foci. Instead, a more direct method would be to isolate Vx3 vesicles by density gradient ultracentrifugation. Analyzing Vx3 vesicles directly may help reduce the ambiguity of whether the identified proteins are associated with Vx3 that is freely diffused or accumulated in foci.

The methods explored to modify Vx3 for reversible binding may also be applied to other sensors and inhibitors. Using 2UbK0 in a CID system, in particular, can be useful for other Ub-binding sensors that are based on UIMs. The rapamycin system with 2UbK0 can be used for in vitro experiments. The DD system is typically used to tune protein expression levels by titrating Shield1 to stabilize a desired amount of target proteins. In disabling Vx3, the DD system was used for its degradation function. By fusing DD to any genetically encoded sensors, bound targets can be reversibly released.

Currently, it is not known whether the K63-polyubiquitinated proteins (e.g. TfR) enter the lysosome to be degraded or are destined to the plasma membrane for secretion. DD-Vx3 would be useful in these experiments to monitor the fate of cargo proteins. As the ubiquitinated proteins are released from Vx3 and continue with downstream processes, their next destinations can be monitored. If they are destined for unconventional secretion to the plasma membrane, Vx3 may intersect with the misfolding-associated protein secretion (MAPS) pathway. During MAPS, a subset of misfolded cytosolic proteins is delivered to lysosomes and then trafficked to the plasma membrane for secretion from the cell.<sup>24,25</sup> The transmembrane proteins that Vx3 binds may occupy the membrane of MAPS vesicles. MAPS is mediated by DNAJC5, a chaperone identified in LC-MS/MS. If TfR and other K63-polyubiquitinated transmembrane proteins are on MAPS vesicles, it's possible that K63-polyUb doesn't modify proteins that are misfolded

themselves but may instead be unconventionally secreted because they occupy vesicles that carry misfolded cytoplasmic proteins.

It is interesting that TfR was unconventionally trafficked because many disease-related proteins do so as well such as in Alzheimer's disease, autoimmune diseases, and diabetes.<sup>46</sup> For example, cystic fibrosis transmembrane conductance regulator (CFTR) could serve as a model substrate in continuing Vx3 foci studies. CFTR is not expressed in HeLa cells,<sup>47</sup> but if it were, CFTR may have co-IPed with Vx3 because misfolded CFTR, especially mutant CFTR  $\Delta F508$ , is unconventionally secreted and chaperones DNAJC5 and HSP90 (another chaperone identified in LC-MS/MS) are involved in its turnover.<sup>48-50</sup>

Further understanding of Vx3 foci may reveal insights into ATG9A function and the underlying mechanisms of a new quality control pathway that involves K63-polyUb. This pathway may potentially be important for disease-related transmembrane proteins with trafficking defects. While this thesis only begins to characterize Vx3 foci, additional studies will expand to identifying the E3 ligase(s) responsible, interacting proteins, and DUBs as they may all play a role in this unique quality control pathway.

## BIBLIOGRAPHY

- 1 Komander, D. & Rape, M. The ubiquitin code. *Annual Review of Biochemistry* **81**, 203-229, doi: 10.1146/annurev-biochem-060310-170328 (2012).
- 2 Pickart, C. M. & Fushman, D. Polyubiquitin chains: polymeric protein signals. *Curr Opin Chem Biol* **8**, 610-616, doi:10.1016/j.cbpa.2004.09.009 (2004).
- 3 Erpapazoglou, Z., Walker, O. & Haguenaer-Tsapis, R. Versatile roles of k63-linked ubiquitin chains in trafficking. *Cells* **3**, 1027-1088, doi:10.3390/cells3041027 (2014).
- 4 Kwon, Y. T. & Ciechanover, A. The Ubiquitin Code in the Ubiquitin-Proteasome System and Autophagy. *Trends in Biochemical Sciences* **42**, 873-886, doi:10.1016/j.tibs.2017.09.002 (2017).
- 5 Sims, J. J. *et al.* Polyubiquitin-sensor proteins reveal localization and linkage-type dependence of cellular ubiquitin signaling. *Nature Methods* **9**, 303-U122, doi:10.1038/nmeth.1888 (2012).
- 6 Dikic, I. & Elazar, Z. Mechanism and medical implications of mammalian autophagy. *Nature Reviews Molecular Cell Biology* **19**, 349-364, doi:10.1038/s41580-018-0003-4 (2018).
- 7 Orsi, A. *et al.* Dynamic and transient interactions of Atg9 with autophagosomes, but not membrane integration, are required for autophagy. *Mol Biol Cell* **23**, 1860-1873, doi:10.1091/mbc.E11-09-0746 (2012).
- 8 Noda, T. Autophagy in the context of the cellular membrane-trafficking system: the enigma of Atg9 vesicles. *Biochemical Society Transactions* **45**, 1323-1331, doi:10.1042/bst20170128 (2017).
- 9 Imai, K. *et al.* Atg9A trafficking through the recycling endosomes is required for autophagosome formation. *Journal of Cell Science* **129**, 3781-3791, doi:10.1242/jcs.196196 (2016).
- 10 Barbieri, M. A., Li, G. P., Mayorga, L. S. & Stahl, P. D. Characterization of Rab5:Q79L-stimulated endosome fusion. *Archives of Biochemistry and Biophysics* **326**, 64-72, doi:10.1006/abbi.1996.0047 (1996).
- 11 Udeshi, N. D., Mertins, P., Svinkina, T. & Carr, S. A. Large-scale identification of ubiquitination sites by mass spectrometry. *Nature Protocols* **8**, 1950-1960, doi:10.1038/nprot.2013.120 (2013).

- 12 Grant, B. D. & Donaldson, J. G. Pathways and mechanisms of endocytic recycling. *Nature Reviews Molecular Cell Biology* **10**, 597-608, doi:10.1038/nrm2755 (2009).
- 13 van Endert, P. Intracellular recycling and cross-presentation by MHC class I molecules. *Immunological Reviews* **272**, 80-96, doi:10.1111/imr.12424 (2016).
- 14 Ritorto, M. S. *et al.* Screening of DUB activity and specificity by MALDI-TOF mass spectrometry. *Nat Commun* **5**, 4763, doi:10.1038/ncomms5763 (2014).
- 15 Freeze, H. H. & Kranz, C. Endoglycosidase and glycoamidase release of N-linked glycans. *Current protocols in protein science* **Chapter 12**, Unit12.14-Unit12.14, doi:10.1002/0471140864.ps1204s62 (2010).
- 16 Busija, A. R., Patel, H. H. & Insel, P. A. Caveolins and cavins in the trafficking, maturation, and degradation of caveolae: implications for cell physiology. *American Journal of Physiology-Cell Physiology* **312**, C459-C477, doi:10.1152/ajpcell.00355.2016 (2017).
- 17 Chaudhary, N. *et al.* Endocytic Crosstalk: Cavins, Caveolins, and Caveolae Regulate Clathrin-Independent Endocytosis. *Plos Biology* **12**, doi:10.1371/journal.pbio.1001832 (2014).
- 18 Ghosh, D. *et al.* VAMP7 regulates constitutive membrane incorporation of the cold-activated channel TRPM8. *Nature Communications* **7**, doi:10.1038/ncomms10489 (2016).
- 19 Ruggiano, A., Foresti, O. & Carvalho, P. ER-associated degradation: Protein quality control and beyond. *Journal of Cell Biology* **204**, 868-878, doi:10.1083/jcb.201312042 (2014).
- 20 Houck, S. A. & Cyr, D. M. Mechanisms for quality control of misfolded transmembrane proteins. *Biochimica Et Biophysica Acta-Biomembranes* **1818**, 1108-1114, doi:10.1016/j.bbamem.2011.11.007 (2012).
- 21 Houck, S. A. *et al.* Quality Control Autophagy Degrades Soluble ERAD-Resistant Conformers of the Misfolded Membrane Protein GnRHR. *Molecular Cell* **54**, 166-179, doi:10.1016/j.molcel.2014.02.025 (2014).
- 22 Fregno, I. *et al.* ER-to-lysosome-associated degradation of proteasome-resistant ATZ polymers occurs via receptor-mediated vesicular transport. *Embo Journal* **37**, doi:10.15252/emj.201899259 (2018).
- 23 Omari, S. *et al.* Noncanonical autophagy at ER exit sites regulates procollagen turnover. *Proceedings of the National Academy of Sciences of the United States of America* **115**, E10099-E10108, doi:10.1073/pnas.1814552115 (2018).

- 24 Lee, J. *et al.* Secretion of misfolded cytosolic proteins from mammalian cells is independent of chaperone-mediated autophagy. *Journal of Biological Chemistry* **293**, 14359-14370, doi:10.1074/jbc.RA118.003660 (2018).
- 25 Xu, Y. *et al.* DNAJC5 facilitates USP19-dependent unconventional secretion of misfolded cytosolic proteins. *Cell Discovery* **4**, doi:10.1038/s41421-018-0012-7 (2018).
- 26 Kaiser, S. E. *et al.* Protein standard absolute quantification (PSAQ) method for the measurement of cellular ubiquitin pools. *Nature Methods* **8**, 691-U129, doi:10.1038/nmeth.1649 (2011).
- 27 Young, A. R. J. *et al.* Starvation and ULK1-dependent cycling of mammalian Atg9 between the TGN and endosomes. *Journal of Cell Science* **119**, 3888-3900, doi:10.1242/jcs.03172 (2006).
- 28 Fegan, A., White, B., Carlson, J. C. T. & Wagner, C. R. Chemically Controlled Protein Assembly: Techniques and Applications. *Chemical Reviews* **110**, 3315-3336, doi:10.1021/cr8002888 (2010).
- 29 Rivera, V. M. *et al.* A humanized system for pharmacologic control of gene expression. *Nat Med* **2**, 1028-1032 (1996).
- 30 Banaszynski, L. A., Liu, C. W. & Wandless, T. J. Characterization of the FKBP.rapamycin.FRB ternary complex. *J Am Chem Soc* **127**, 4715-4721, doi:10.1021/ja043277y (2005).
- 31 Putyrski, M. & Schultz, C. Protein translocation as a tool: The current rapamycin story. *Febs Letters* **586**, 2097-2105, doi:10.1016/j.febslet.2012.04.061 (2012).
- 32 Liang, J., Choi, J. & Clardy, J. Refined structure of the FKBP12-rapamycin-FRB ternary complex at 2.2 Å resolution. *Acta Crystallogr D Biol Crystallogr* **55**, 736-744 (1999).
- 33 Sims, J. J. & Cohen, R. E. Linkage-specific avidity defines the lysine 63-linked polyubiquitin binding preference of Rap80. *Mol Cell* **33**, 775-783, doi:10.1016/j.molcel.2009.02.011 (2009).
- 34 Rossi, A. M. & Taylor, C. W. Analysis of protein-ligand interactions by fluorescence polarization. *Nature Protocols* **6**, doi:10.1038/nprot.2011.305 (2011).
- 35 Kim, Y. C. & Guan, K.-L. mTOR: a pharmacologic target for autophagy regulation. *Journal of Clinical Investigation* **125**, 25-32, doi:10.1172/jci73939 (2015).
- 36 Morita, E., Arii, J., Christensen, D., Votteler, J. & Sundquist, W. I. Attenuated protein expression vectors for use in siRNA rescue experiments. *Biotechniques* **0**, 1-5, doi:10.2144/000113909 (2012).

- 37 Ouyang, H. *et al.* Protein Aggregates Are Recruited to Aggresome by Histone Deacetylase 6 via Unanchored Ubiquitin C Termini. *Journal of Biological Chemistry* **287**, 2317-2327, doi:10.1074/jbc.M111.273730 (2012).
- 38 Miyamoto, T. *et al.* Rapid and orthogonal logic gating with a gibberellin-induced dimerization system. *Nature Chemical Biology* **8**, 465-470, doi:10.1038/nchembio.922 (2012).
- 39 Kopytek, S. J., Standaert, R. F., Dyer, J. C. & Hu, J. C. Chemically induced dimerization of dihydrofolate reductase by a homobifunctional dimer of methotrexate. *Chem Biol* **7**, 313-321 (2000).
- 40 Banaszynski, L. A., Chen, L. C., Maynard-Smith, L. A., Ooi, A. G. L. & Wandless, T. J. A rapid, reversible, and tunable method to regulate protein function in living cells using synthetic small molecules. *Cell* **126**, 995-1004, doi:10.1016/j.cell.2006.07.025 (2006).
- 41 Chu, B. W., Banaszynski, L. A., Chen, L. C. & Wandless, T. J. Recent progress with FKBP-derived destabilizing domains. *Bioorganic & Medicinal Chemistry Letters* **18**, 5941-5944, doi:10.1016/j.bmcl.2008.09.043 (2008).
- 42 Los, G. V. *et al.* HaloTag: A novel protein labeling technology for cell imaging and protein analysis. *Acs Chemical Biology* **3**, 373-382, doi:10.1021/cb800025k (2008).
- 43 Grimm, J. B. *et al.* Bright photoactivatable fluorophores for single-molecule imaging. *Nature Methods* **13**, 985-+, doi:10.1038/nmeth.4034 (2016).
- 44 Shcherbakova, D. M. & Verkhusha, V. V. Near-infrared fluorescent proteins for multicolor in vivo imaging. *Nature Methods* **10**, 751-+, doi:10.1038/nmeth.2521 (2013).
- 45 Pickart, C. M. & Raasi, S. Controlled synthesis of polyubiquitin chains. *Ubiquitin and Protein Degradation, Pt B* **399**, 21-36, doi:10.1016/s0076-6879(05)99002-2 (2005).
- 46 Kim, J., Gee, H. Y. & Lee, M. G. Unconventional protein secretion - new insights into the pathogenesis and therapeutic targets of human diseases. *Journal of Cell Science* **131**, doi:10.1242/jcs.213686 (2018).
- 47 Denning, G. M., Ostedgaard, L. S., Cheng, S. H., Smith, A. E. & Welsh, M. J. LOCALIZATION OF CYSTIC-FIBROSIS TRANSMEMBRANE CONDUCTANCE REGULATOR IN CHLORIDE SECRETORY EPITHELIA. *Journal of Clinical Investigation* **89**, 339-349, doi:10.1172/jci115582 (1992).
- 48 Noh, S. H. *et al.* Specific autophagy and ESCRT components participate in the unconventional secretion of CFTR. *Autophagy* **14**, 1761-1778, doi:10.1080/15548627.2018.1489479 (2018).

- 49 Aversa, M. *et al.* Calpain digestion and HSP90-based chaperone protection modulate the level of plasma membrane F508del-CFTR. *Biochimica Et Biophysica Acta-Molecular Cell Research* **1813**, 50-59, doi:10.1016/j.bbamcr.2010.11.008 (2011).
- 50 Schmidt, B. Z., Watts, R. J., Aridor, M. & Frizzell, R. A. Cysteine String Protein Promotes Proteasomal Degradation of the Cystic Fibrosis Transmembrane Conductance Regulator (CFTR) by Increasing Its Interaction with the C Terminus of Hsp70-interacting Protein and Promoting CFTR Ubiquitylation. *Journal of Biological Chemistry* **284**, 4168-4178, doi:10.1074/jbc.M806485200 (2009).
- 51 Yamamoto, H. *et al.* Atg9 vesicles are an important membrane source during early steps of autophagosome formation. *Journal of Cell Biology* **198**, 219-233, doi:10.1083/jcb.201202061 (2012).
- 52 Ran, F. A. *et al.* Genome engineering using the CRISPR-Cas9 system. *Nature Protocols* **8**, 2281-2308, doi:10.1038/nprot.2013.143 (2013).
- 53 Nageswaran, S. *et al.* CRISPR Guide RNA Cloning for Mammalian Systems. *Jove-Journal of Visualized Experiments*, doi:10.3791/57998 (2018).
- 54 Chari, R., Yeo, N. C., Chavez, A. & Church, G. M. sgRNA Scorer 2.0: A Species-Independent Model To Predict CRISPR/Cas9 Activity. *Acs Synthetic Biology* **6**, 902-904, doi:10.1021/acssynbio.6b00343 (2017).

## APPENDIX 1: ENDOGENOUSLY-TAG ATG9A BY CRISPR

### A1.1 Introduction

Many of the experiments utilizing HeLa cells stably expressing 3xFLAG-Vx3-EGFP under a Dox-inducible promoter also required staining for ATG9A using antibodies. In order to visualize ATG9A during live-cell imaging, ATG9A was overexpressed as a fusion to a fluorescent protein. However, it is known that overexpressed ATG9A displays aberrant behavior such as formation of immobile foci at the Golgi apparatus.<sup>51</sup> In order to reduce complications for studying Vx3 foci with ATG9A during live-cell imaging, a cell line with ATG9A endogenously tagged with myc-HaloTag-TEV at the N-terminus was created.

### A1.2 Materials and methods

#### *A1.2.1 CRISPR/Cas9-mediated genome editing*

Knock-in cells were created following published methods<sup>52,53</sup>. To create the donor plasmid, a pUC19 plasmid was modified to contain the tags myc-HaloTag-TEV flanked by 500-700 bp homology arms. The tag was targeted for homologous recombination using three guide RNAs designed using the Zhang Lab's CRISPR design tool<sup>52</sup> and the Church lab's sgRNA Scorer 2.0<sup>54</sup>. The guide sequences 5'-GCGCCTAGAGGCCTCCTATA-3', 5'-TTATTGGCAGGTGGTCAAGG-3', and 5'-TGATTCACCCCAGGGGAGG-3' were cloned into pSpCas9(BB)-2A-GFP (PX458), a gift from Feng Zhang (Addgene plasmid #48138, Massachusetts Institute of Technology). For each Cas9 plasmid containing a guide sequence, a new donor plasmid was cloned by mutating the corresponding PAM sequence in the homology arms. HeLa Vx3#6 3xFLAG-Vx3-EGFP stable cells were seeded in 6 cm dishes and separately transfected with 2.75 µg of each Cas9 plasmid and 2.75 µg of the corresponding donor plasmid

using Lipofectamine 3000 (Thermo Fisher) according to manufacturer's instructions. After 48 h transfection, the cells transfected with different Cas9 plasmids were pooled together and FACS-sorted for the 10% highest EGFP-expressing cells. Dox was not added to induce for Vx3-EGFP expression, so the EGFP signal mainly came from Cas9-EGFP. The cells were sorted on a BD FACSAria III (BD Biosciences) using sorting buffer (25 mM HEPES pH 7.5, 2% FBS, 2 mM EDTA in HBSS) and collected in sorting media (25 mM HEPES pH 7.5, 20% FBS, 100 U/mL penicillin-streptomycin, 2 mM L-glutamine in DMEM).

#### *A1.2.2 Microscopy*

Cells were labeled with 100 nM JF646-HaloTag ligand, a gift from Luke Davis (Howard Hughes Medical Institute) and then imaged using live-cell imaging conditions described in Chapter 3.

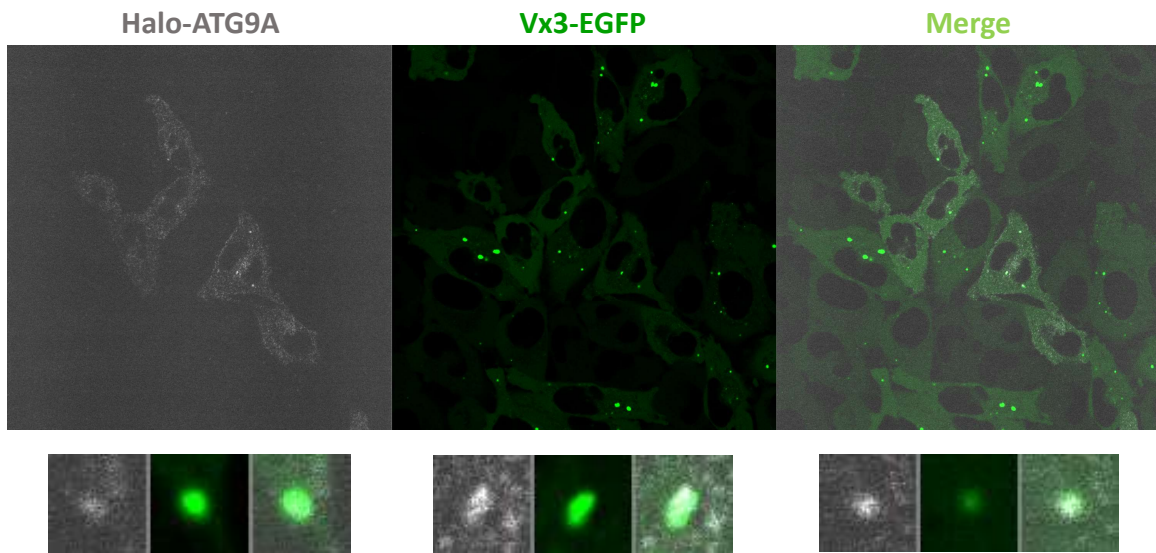


**FIG A1.1 Endogenously-tagged ATG9A in Vx3-EGFP cells.** After the cells recovered from FACS, they were induced with 1  $\mu\text{g}/\text{mL}$  Dox for 48 h and labeled with JF-646-HaloTag. Cells that are edited express ATG9A with an N-terminal myc-HaloTag-TEV at the endogenous locus. Although edited ATG9A co-localized well with Vx3 foci, the low levels of endogenous ATG9A yield a very dim fluorescent signal.

## APPENDIX 2: RAPAMYCIN SYSTEM CONSTRUCTS

### FRB-Vx3

MPSSHHHHHHSSGLVPRGSHMEESILWHEMWHEGLEEASRLYFGERNVKGMFEVLEPLHAMMERGPQTLK  
ETSFNQAYGRDLMEAQEWCRKYMKSGNVKDLLQAWDLYYHVFRRISEEEEDPDLKAAIQESLREARAEK  
VKEDEEELIRKAIELSLKESREVNAAQEEDDEEELIRKAIELSLKECRNSA

### UbK0-FKBP12

MGSSHHHHHHSSGLVPRGSHMQIFVRTLGTGRITITLEVEPSDTIENVRARIQDREGIPPDQORLI FAGRQL  
EDGRTLSDYNIQRESTLHLVLRRLRGVPASRI PNDLRQRMRGVQVETISPGDGRTFPKRGQTCVVHYTGML  
EDGKKFDSSRDRNKPFKFM LGKQEVIRGWEEGVAQMSVGQRAKLTISPDYAYGATGHPGIIPPHATLVFD  
VELLKLET

### 2UbK0-FKBP12

MGSSHHHHHHSSGLVPRGSHMQIFVRTLGTGRITITLEVEPSDTIENVRARIQDREGIPPDQORLI FAGRQL  
EDGRTLSDYNIQRESTLHLVLRRLRGVSGMQIFVRTLGTGRITITLEVEPSDTIENVRARIQDREGIPPDQOR  
LIFAGRQLEDGRTLSDYNIQRESTLHLVLRRLRGVPGSGSGPASRI PNDLRQRMRGVQVETISPGDGRTFP  
KRGQTCVVHYTGML EDGKKFDSSRDRNKPFKFM LGKQEVIRGWEEGVAQMSVGQRAKLTISPDYAYGATG  
HPGIIPPHATLVFDVELLKLET

**FIG A2.1 Vx3 rapamycin system constructs.** The protein sequences start with a 6xHis-tag and are color coded with FRB in green, Vx3 in blue, Ubk0 in yellow, and FKBP12 in red.

## LIST OF ABBREVIATIONS

A.U.	Arbitrary units
BSA	Bovine serum albumin
CID	Chemically-induced dimerization
CRISPR	Clustered regularly interspaced short palindromic repeats
DAPI	4',6-diamidino-2-phenylindole
DD	Destabilizing domain
DMEM	Dulbecco's modified Eagle medium
DMSO	Dimethyl sulfoxide
Dox	Doxycycline
DTT	Dithiothreitol
DUB	Deubiquitinating enzyme
ER	Endoplasmic reticulum
FT	Flow through
IB	Immunoblotting
IP	Immunoprecipitation
IPTG	Isopropyl $\beta$ -D-1-thiogalactopyranoside
JF	Janelia Fluor
LC-MS/MS	Liquid chromatography tandem mass spectrometry
MAPS	Misfolding-associated protein secretion
pA	Photoactivatable
PAM	Protospacer adjacent motif

PBS	Phosphate buffered saline
PCR	Polymerase chain reaction
PMSF	Phenylmethylsulfonyl fluoride
RIPA	Radioimmunoprecipitation assay
SB	Sample buffer
SC	Spectral count
SDS-PAGE	Sodium dodecyl sulfate-polyacrylamide gel electrophoresis
sgRNA	Short guide ribonucleic acid
siRNA	Small interfering ribonucleic acid
TBS	Tris buffered saline
TCEP	Tris(2-carboxyethyl)phosphine hydrochloride
Tf	Transferrin
UIM	Ubiquitin interacting motif
Vx3NB	Vx3 non-binding mutant
Ub	Ubiquitin